FATE AND TRANSPORT OF POLLUTANTS AND THEIR IMPACTS ON THE ALA WAI CANAL

A THESIS SUBMITTED TO THE GRADUATE DIVISION OF THE UNIVERSITY OF HAWAIʻI AT MĀNOA IN PARTIAL FULFILLMENT OF THE REQUIREMENTS FOR THE DEGREE OF
MASTER OF SCIENCE
IN
CIVIL ENGINEERING

AUGUST 2011

By
Benjamin J. Card

Thesis Committee:
Clark Liu, Chairperson
Roger Babcock
Tao Yan

Acknowledgments

I would like to take this opportunity to thank all those who made the completion of this report possible. In particular I would like to thank my advisor Professor Clark Liu for his guidance and support throughout this entire study. I am also grateful to Professors Roger Babcock and Tao Yan for their willingness to serve on my committee.

My colleagues Krispin Fernandez and Tsu-Chuan Lee are also deserving of recognition for their contributions to this project. Krispin's surface water model of the inputs into the canal was instrumental to the creation of all the models discussed within this paper. Tsu-Chuan was also a big help to this project by providing help with much of the lab work that was required.

This project was financed by the Hawaii Department of Transportation as a part of a survey and modeling analysis project of their storm water runoff. The collection and analysis of dissolved oxygen and chlorophyll data was made possible by the use of the Water Resource Research Center's vehicles and the civil engineering department's laboratory facility.

Abstract

A water quality model was developed to simulate the fate and transport of nutrients within the Ala Wai Canal and to evaluate the impacts of storm runoff on the canal's biological activity. The hydraulic component of the model was developed by considering the canal as a series of four completely stirred tank reactors (CSTRs), with flushing time as the key hydraulic parameter. Flushing time represents the average time that a particle of freshwater will remain in the estuary. The flushing times were estimated based on salinity data collected by this study and other previous studies.

Modeling results indicated that the Total Maximum Daily Load (TMDL) of total nitrogen, which has been set by the state as 25 kg/day, was exceeded by both the wet and dry season averages. This 25 kg/day limit was based on state water quality standards for the canal that state the nitrogen concentration within the canal should not exceed 200µg/l. Using parameters that have been updated since the TMDL study such as the background concentration of nitrogen, flushing time, and volume of the canal, it was also determined that the water quality standard for total nitrogen of 200µg/L was exceeded within certain areas of the canal.

Field data of chlorophyll *a* concentrations were collected over a two month period to provide a base for model testing and calibration. Modeling analysis suggests that the canal is highly productive and that this production increases after increased loading of nutrients following a rainstorm. A final application of this model was

discussed that showed its potential to determine the fate of contaminants from possible biological spills within the canal.

Field data of diurnal dissolved oxygen and chlorophyll *a* concentrations were collected to determine if the model's conclusions on the health of the canal were correct. Field data suggested that the canal is highly productive and can be classified as eutrophic. This bioproductivity was shown to greatly increase after storm events.

Table of Contents

List of Tables

List of Figures

Introduction

Background Information/Literature Review

The Ala Wai Canal is a manmade estuary constructed in 1927 by the Army Corps of Engineers. The canal is approximately 3100 meters long from its head near Kapahulu Avenue to its mouth that flows into Mamala Bay. The surface area of the canal is roughly 2 x 10^5 m^2 and it was originally dredged to depths of 3-6 meters (Gonzalez, 1971). However, heavy sedimentation has reduced the depths of the canal and it has therefore been dredged again multiple times the most recent being in 2002. It is composed mostly of seawater that flows in from Mamala Bay, but also contains freshwater from inflowing rivers, storm drains, and storm runoff from the surrounding areas. The two major sources of freshwater into the canal are the Mānoa-Palolo Drainage Canal and Makiki Stream. These two sources contribute the majority of freshwater to the canal, but runoff from the Ala Wai Golf Course, Honolulu Zoo, Waikiki, and other surrounding areas also contribute to the volume of freshwater within the canal.

Because the canal drains much of the runoff from Waikiki, Mānoa, Makiki, and other surrounding areas its waters contain much of the nutrients found in surface water runoff. Two nutrients that are of concern and discussed within this paper are nitrogen and phosphorus. These nutrients are carried by the surface runoff into the canal where they accumulate until they either flow out of the canal and into the bay or are used for growth by organisms living in the canal. Nitrogen and phosphorus are often rate limiting nutrients in the growth of marine microorganisms. Their abundance allows

these microorganisms' populations to expand causing negative environmental effects. The relatively high levels of nitrogen and phosphorus within the canal have placed the canal in a eutrophic state (Laws et al. 1993). The effects of this eutrophication can be seen by the canal's high nutrient levels, excessive algal biomass (Harris, 1972; Laws, 1994), and low oxygen levels in its bottom waters (Gonzalez, 1971; Laws, 1994; Miller, 1975).

The Ala Wai Canal has faced eutrophication problems for decades and many studies have been undertaken to diagnose when and where the problem occurs within the canal. A study completed in 1972 titled "Primary Production in a Small Tropical Estuary" focused on the productivity of the estuary and the limiting aspects of the process. The study measured production by the carbon-14 method, pigment concentrations, suspended particulate matter, light attenuation, and nitrate and phosphate concentrations over a 13 month period. The study found that there were high production indices that reached 17 suggesting that the production within the canal is non-nutrient limited. The two major factors influencing primary production within the canal were instead determined to be flushing time and suspended particulate matter that blocked out incoming light (Harris, 1972). It was also determined that both production and biomass increased the further from the mouth of the canal the measurements were taken.

A study similar to Harris's 1972 study was carried out by a team run by Professor Edward Laws of the University of Hawai'i in 1992. This study looked at much of the same data, but with more sampling stations over a shorter time period. It was found

that nitrogen and carbon concentrations increased from the mouth to the head of the estuary. Chlorophyll *a* concentrations and photosynthetic rates were also found to increase from the mouth to the head of the estuary. These patterns and the raw data were similar to those reported in the 1972 study by Harris. From this it was concluded that despite dredging and changes in depth that the conditions in the estuary did not change much in the 20 years between the studies (Laws et al. 1994).

Dissolved oxygen levels within the canal have also been documented for decades with the fear that the canal's high levels of productivity will deplete its dissolved oxygen content to dangerous levels. A study completed in 1971 by Frank Gonzalez attempted to document the physical and chemical features of the canal. One of the features observed was the dissolved oxygen levels. The study concluded that the longitudinal sections of the canal exhibit roughly the same dissolved oxygen pattern. That is there are generally high concentrations of dissolved oxygen at the entrance of a freshwater stream, relatively uniform concentrations at intermediate depths, and very low concentrations at the deepest depths of the canal (Gonzalez, 1971). The study also found that dissolved oxygen levels approached zero in the bottom waters towards the head of the canal.

Laws et al. (1994) studied the diel pattern of dissolved oxygen along the canal for two six week periods during the summers of 1991 and 1992. The study found that the canal displayed the expected variation in diel oxygen patterns. The greatest variation in diel dissolved oxygen levels were found to occur at the head of the estuary with the least variation at the mouth. At the head of the estuary it was found that the upper

meter of water was supersaturated with oxygen by the end of the day while by daybreak the bottom waters' O_2 concentrations had dropped to 2-4 mg liter^{-1} (Laws et al. 1994). The diel dissolved oxygen readings for this study did not however record any data below two meters. There were some readings that took place during daylight hours at three meters that showed dissolved oxygen levels that were above saturation. However, based on the diel pattern of dissolved oxygen taken in this study and the data from Gonzalez (1971), it was concluded that EPA water quality criteria appeared to be violated at depths below three meters especially at night (Laws et al. 1994).

One final study that recorded dissolved oxygen levels within the canal was completed in 1975 by Jacquelin Miller. This study recorded dissolved oxygen data at 38 locations along the canal for a period of 15 months. The study yielded no conclusive results displaying seasonal variation in dissolved oxygen levels, and noted that daily variations were much greater than seasonal changes. The study also stated that tidal direction has a minimal influence on the distribution of dissolved oxygen both horizontally and vertically. Several of the stations near the back of the canal were also reported to have mean dissolved oxygen concentrations below 2ppm at their bottom depth (Miller, 1975).

These past studies have thoroughly researched dissolved oxygen levels in the canal with attempts to show any patterns in seasonal, tidal, diel, or spatial variation. It is clear that there is variation between dissolved oxygen levels at varying depths (Gonzalez, 1971; Miller, 1975; Laws et al. 1993) as well as a distinct diel pattern (Laws et al. 1994). What is not known is how low the oxygen levels currently get at the deeper

areas of the canal. Miller documented average levels of dissolved oxygen approaching zero at some points of the canal. However, where those measurements were taken may no longer be that deep due to sedimentation, and there is the possibility that the water quality has changed since the 1975 study. It would therefore be beneficial to obtain current measurements that document the areas that are most susceptible to oxygen depletion.

As stated previously the nutrient levels in the canal have generally been measured well above levels associated with nutrient limitation (Harris, 1972; Laws et al. 1994). This means that there is an excess of nutrients in the canal allowing microbial growth to occur at extremely high levels. This is because the Ala Wai Canal is one of the most heavily fertilized estuaries in the world (Laws et al. 1993). The concentrations of nitrogen and phosphorus are also even higher after storm events from increased levels of runoff (Laws et al. 1994). Because high levels of nitrogen and phosphorus are known to lead to eutrophic conditions and the general poor health of a receiving water body discussed previously, the amount of nutrient loading into the canal has become important to the city of Honolulu and the state of Hawai‘i.

In an attempt to quantify and control the levels of phosphorus and nitrogen within the canal the state has designated total maximum daily loads (TMDLs) of each pollutant into the canal. The state originally developed a TMDL report for the canal in 1995 and then revised that plan in 2002. The original TMDLs adopted in 1995 were based on a 1993 TMDL report completed by William Freeman. The original report used two methods to determine the TMDLs for the canal.

The first method used the state's water quality standards as numeric targets for both nitrogen and phosphorus in the canal. The targets were 200µg/l for nitrogen and 25µg/l for phosphorus. It then allocated incoming nutrient loads. The canal was assumed to have a background concentration equal to the coastal waters water quality standards. These assumed levels were 150µg/l for nitrogen and 20µg/l for phosphorus. The remaining loads were then determined based on the ALAWAT model which determined the loads from the surrounding land areas. An excess concentration was then determined for each pollutant by adding the daily concentration determined by the ALAWAT model to the background concentration and subtracting the allowable concentration. Using this method it was determined that the excess daily concentrations of nitrogen and phosphorus were 132µg/l and 69µg/l respectively (Freeman, 1993).

The second method used by Freeman relied on the water quality data of the Ala Wai. This method used the average concentrations of each nutrient measured in the canal and subtracted the allowable concentration. This was then divided by the average water residence time to arrive at the average excess daily concentrations. The residence time for water was determined to be 3 days based on a dye test completed by E.K. Noda & Associates in March of 1992. The dye test determined the mean residence time of water in the canal to be between 40-60 hours. By this method the excess daily concentrations were determined to be 137µg/l for nitrogen and 11µg/l for phosphorus (Freeman, 1993).

The results of each method were then averaged because Freeman concluded that neither method was preferable to the other. The excess daily concentrations were then multiplied by the volume of the canal and converted to kilograms/day. The calculated excess daily loads were calculated to be 44kg/day and 13kg/day for nitrogen and phosphorus respectively (HIDOH, 2002).

The 1995 TMDL report was revised in 2002. The results of the 1995 report were not changed; however, the way that they were represented did change. The TMDLs from the 1995 report were restated as allowable mass loads instead of excess loads. Also a 10% unallocated reserve was added to provide a margin of safety. The current TMDLs are 25kg/day for nitrogen and 10kg/day for phosphorus (HIDOH, 2002).

Goals of this project

The overall goal of this project was to determine what effect the varying nutrient levels have on the biological activity of the canal. To do this a water quality model was created. The model was used to determine the distribution of nutrients within the canal. From the modeled concentrations of nutrients it can be determined if the state's water quality standards and TMDL limits are met within the canal. The water quality model was also used to predict the changes in biological activity that would occur from varying levels of available nutrients.

Another goal was to collect field data to calibrate the water quality model and as a check on the overall biological health of the canal. The plan was to not rely solely on the criteria of the water quality standards and TMDL limits to determine whether or not the canal could be deemed healthy. To do this diurnal dissolved oxygen and chlorophyll

a levels were measured within the canal. The dissolved oxygen data was used to determine if any areas of the canal contain oxygen levels that are dangerously low for aquatic life. The dissolved oxygen data was also analyzed to determine the health of each segment based on methods described by Wang et al., (2002) and Liu (1982). The chlorophyll data was used to classify the trophic levels of each of the segments in the canal. Both chlorophyll and dissolved oxygen data were also measured to document any changes that resulted in the canal caused by increased runoff from rainstorms. The dry and wet weather chlorophyll averages were ultimately used to calibrate the water quality model.

The final goal of this project was to show other potential uses for the water quality model. To do this a wastewater spill was modeled within the canal. The flushing times calculated for the water quality model were used to predict bacteria concentrations in each effected segment over time.

Significance of Work

The receiving water model was created as a way to predict the fate and transport of the newly modeled nutrient data, and to improve upon older receiving water models of the canal. Several approaches were used in this model as a way to enhance older models such as the one used for the TMDL report of the canal. First the model incorporates different weather conditions. Dry and wet weather are modeled to represent conditions of both increased runoff from rain, and no rain runoff. Dry and wet seasonal averages are also modeled to give a better understanding of how average conditions change from the dry season to the wet season. The canal was also treated as

a series of CSTRs with different flushing times instead of a single receiving water body. This is important because a particle that enters the canal through runoff from an area such as the zoo at the back of the canal will spend a lot more time in the canal and have a greater impact than one that enters near the mouth of the canal. Another change from previous models is the incorporation of data from Mamala Bay for background nutrient levels. The TMDL report assumed that the background levels were equal to the limits set by the coastal waters water quality standards. This method is good in that it is conservative, but in this case is overly conservative and the actual background levels of nutrients provide a much more accurate picture.

The work on the biological activity within the canal is significant for a number of reasons. Dissolved oxygen levels were measured to determine if certain locations within the canal fall outside the desired range for a healthy aquatic ecosystem. Miller's 1975 study documented that this did occur; however over 35 years have elapsed since that study was conducted. The use of dissolved oxygen and chlorophyll *a* concentrations to classify the health of the canal is also an important check on the modeled nutrients. If the project solely modeled the nutrients and said they were acceptable by state standards then it would be assumed that the conclusion of the report is that the canal is a healthy water body. However, the field data will be an important check to see if the nutrient levels in the canal are in fact at levels that promote a healthy level of bioproductivity.

Field Survey

As part of this project field data for salinity, dissolved oxygen, and chlorophyll were gathered. Salinity data were used in the calculations of the segments' flushing times. Dissolved oxygen data were used to determine the general health of the canal. It was desirable to obtain diurnal dissolved oxygen data for several reasons. One goal was to determine if there were any areas of the canal that contain dissolved oxygen levels that may be dangerously low for aquatic life. Another major goal was to use the diurnal dissolved oxygen patterns of the canal to determine the level of bioproductivity in each of the four segments. The final goal was to document how these levels changed with increased levels of runoff from rain events and any changes that occurred from tidal variations.

Chlorophyll data was also used to determine the level of bioproductivity in the canal. One goal was to determine the trophic level of four segments using chlorophyll *a* measurements from the field. These will be classified by a system given by Wetzel (2001) which states that a water body that contains chlorophyll *a* concentrations that average 2-15 mg m^{-3} can be considered mesotrophic while a water body with averages ranging from 10-500 mg m^{-3} can be considered eutrophic. It was also of interest to see how this was affected by increased runoff and tidal effects. The chlorophyll field data was also used in the creation and calibration of the final Ala Wai water quality model.

Methods

Salinity

Dry weather conditions were chosen to measure salinity data that would be used in the creation of the dry weather flushing time calculations. The measurements were taken with a YSI conductivity meter model # 6920. Measurements were taken on two separate dates at a total of eight locations throughout the canal. The measurements at all eight locations were taken at approximately the midpoint between the two sides of the canal.

Dissolved Oxygen

Diurnal dissolved oxygen readings were taken throughout the month of February in 2011. The readings were taken using a YSI 6920 dissolved oxygen probe that had been tested against Winkler Titration Method for accuracy. Readings were taken at 28 different times throughout the month long period at four different locations. These locations were meant to represent the four segments of the canal that had been created in the hydraulic model of the canal. The four locations can be seen in figure 1. Dissolved oxygen readings were taken at the surface and at varying depths of one meter to a total depth of three meters from the Kalakaua and McCully Street bridges. Readings at the other two sampling areas towards the back of the canal near University Avenue and the Waikiki-Kapahulu library were taken at the surface and a depth of either a half meter or one meter depending on varying depths due to tidal changes.

Sampling was done throughout the day as to achieve diurnal dissolved oxygen data. Of the 28 sampling events 10 were taken at sunrise, 10 at sunset, and the other 8

between noon and 3:30pm. Besides the variation due to biological activity it was also of interest to find if tidal changes or increased runoff due to rain had any documentable effects upon the dissolved oxygen levels in the canal. As such the direction of the tide (incoming or outgoing) and any rain that occurred prior to sampling were noted during each sampling event.

Figure 1. Four sampling locations used in dissolved oxygen study.

Chlorophyll

Chlorophyll *a* samples were collected 12 times during the months of February and March of 2011. All samples were collected from just below the surface from each of the four previously discussed segments. Unlike with dissolved oxygen the chlorophyll samples did not come from the same location within each segment each time. Since the samples were taken from the surface and depth was not an issue, there were more available locations to sample. As such the samples were collected at various points

throughout segments 1, 3, and 4 although because most of the land bordering segment 2 was fenced off on the Mānoa side all samples from that segment were collected from the end of University Avenue. All samples were then stored in a cooler and analyzed using trichromatic method (standard method 10200C) within 24 hours of sampling.

Results

Salinity

The salinity profile and data collected by this study can be viewed in figure 2 and table 1.

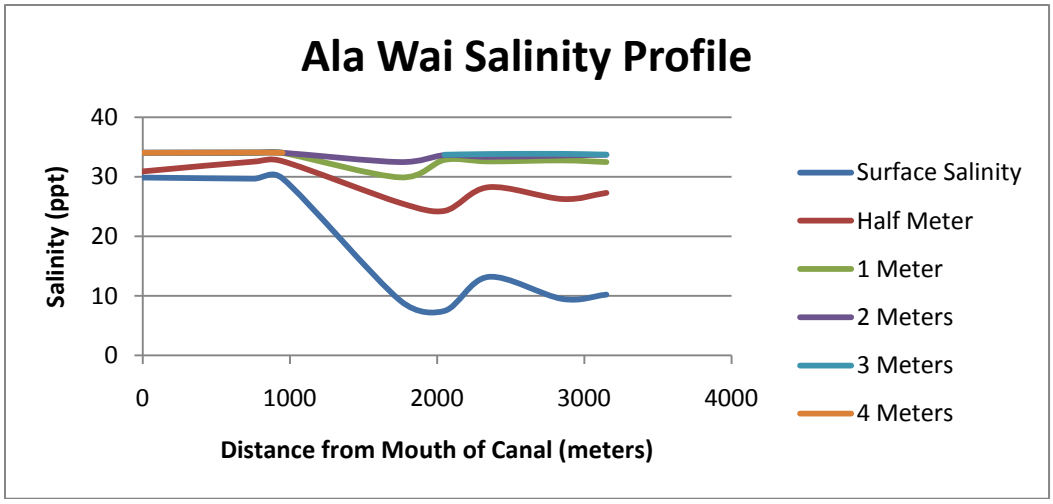

Figure 2. Dry season salinity profile gathered by this study

Table 1. Measured dry season salinity data

Distance from Mouth of Canal (m)	Surface Salinity (ppt)	Half Meter Salinity (ppt)	1 Meter Salinity (ppt)	2 Meters Salinity (ppt)	3 Meters Salinity (ppt)	4 Meters Salinity (ppt)
0	29.87	30.90	30.97	34.04	34.04	34.04
750	29.68	32.54	33.99	34.06	34.07	34.08
950	29.71	32.61	33.99	34.03	34.04	34.04
1750	9.19	25.58	29.89	32.46	-	-
2050	7.48	24.25	32.83	33.63	33.71	-
2250	13.19	28.24	32.57	33.35	33.82	-
2750	9.49	26.25	32.74	33.57	33.85	-
3150	10.21	27.28	32.46	33.70	33.70	-

Dissolved Oxygen

The average dissolved oxygen concentrations can be seen in tables 2-5. The tables list the mean concentration, the number of sampling events, and the standard deviation. All four stations displayed a diurnal pattern of fluctuation with the lowest average concentrations at sunrise and increased concentrations at midday through sunset. Average dissolved oxygen concentrations were also found to decrease with depth. All four segments displayed similar ranges in terms of average variation between sunrise and sunset at the surface waters. Segment one displayed the greatest average range with an average sunrise concentration of 5.51 mg liter^{-1} and an average sunset concentration of 7.90 mg liter^{-1} for an average range of 2.39 mg liter^{-1}. Segments 2-4 had average ranges of 1.83, 1.82, and 2.04 mg liter^{-1} respectively. Maximum ranges for of high and low concentrations showed much more variability than did the averages. The maximum ranges displayed in the surface waters were 8.53, 8.22, 7.66, and 7.14 mg liter^{-1} for segments 1-4 respectively. When including the bottom waters these ranges increased to 10.26, 9.83, 8.68, and 8.41 mg liter^{-1} for segments 1-4 respectively. Overall the highest value of dissolved oxygen for the canal was measured at 12.54 mg liter^{-1} with the lowest value being 1.71 mg liter^{-1}. The complete dissolved oxygen data can be viewed in appendix C.

Table 2. Average dissolved oxygen (mg liter^{-1}) measured from segment 1.

Depth	6:00 – 7:30	12:00 – 14:00	14:00 – 15:30	17:00 – 20:00
Surface	5.51 (10) ±1.21	6.61 (7) ± 2.24	11.97 (1)	7.90 (10) ± 2.29
Half Meter	4.83 (2) ± 0.25	NA	NA	10.51 (2) ± 1.57
One Meter	4.17 (5) ± 0.90	4.89 (3) ± 2.55	7.07 (1)	7.32 (5) ± 1.08

Table 3. Average dissolved oxygen (mg liter^{-1}) measured from segment 2.

Depth	6:00 – 7:30	12:00 – 14:00	14:00 – 15:30	17:00 – 20:00
Surface	6.48 (10) ± 1.36	7.80 (5) ± 1.76	9.51 (3) ± 2.41	8.31 (10) ± 2.36
Half Meter	5.13 (6) ± 1.94	8.21 (1)	7.40 (2) ± 1.8	7.74 (10) ± 1.75

Table 4. Average dissolved oxygen (mg liter^{-1}) measured from segment 3.

Depth	6:00 – 7:30	12:00 – 14:00	14:00 – 15:30	17:00 – 20:00
Surface	6.78 (10) ± 1.08	7.33 (7) ± 1.41	11.76 (1)	8.60 (10) ± 1.93
One Meter	5.82 (10) ± 0.94	5.99 (7) ± 1.27	9.61 (1)	8.09 (10) ± 1.71
Two Meters	5.22 (10) ± 1.10	5.53 (7) ± 1.07	8.27 (1)	6.90 (10) ± 1.56
Three Meters	5.07 (10) ± 1.00	5.09 (7) ± 1.26	6.81 (1)	5.91 (10) ± 1.3

Table 5. Average dissolved oxygen (mg liter^{-1}) measured from segment 4.

Depth	6:00 – 7:30	12:00 – 14:00	14:00 – 15:30	17:00 – 20:00
Surface	6.69 (10) ± 1.10	7.6 (6) ± 1.76	9.88 (2) ± 3.17	8.73 (10) ± 1.83
One Meter	6.14 (10) ± 0.97	6.68 (6) ± 1.39	7.59 (2) ± 3.22	8.23 (10) ± 1.57
Two Meters	5.49 (10) ± 1.00	5.94 (6) ± 1.31	6.58 (2) ± 2.31	7.24 (10) ± 1.44
Three Meters	5.24 (10) ± 1.04	5.07 (6) ± 1.38	6.03 (2) ± 1.44	6.24 (10) ± 1.45

Effect of Increased Runoff

There were no major storms during the sampling period. There were however, plenty of instances where small amounts of rain would occur somewhere in the contributing land area to the canal. A problem arose when trying to define wet and dry weather from these situations. An hour's worth of rain that only covered a portion of the contributing area could not be considered a storm event, but neither could it be considered dry weather. Because of this dilemma a simple method was used to determine wet or dry weather. If it rained for more than an hour in the lower Mānoa area than the canal conditions were considered wet for the next two days (chosen to match the calculated flushing time). Because of the ambiguity involved in this no strong statistical conclusions could be made when comparing wet vs. dry weather patterns.

It was clear even without a strong definition of wet vs. dry weather that dissolved oxygen levels were generally lower following a rain event. In particular one rain event deposited large amounts of sediment into the canal. TSS measurements were not made, but this was obvious with the naked eye as the entire canal turned brown and visibility into the canal became very low for two days. This rain event occurred on the night of February 19th. Diurnal readings were taken from the morning of the 18th through the afternoon of the 21st. This rain event resulted in the lowest dissolved oxygen readings that were taken during this testing period the lowest of which was a reading of 1.71 mg liter^{-1} recorded in segment 1. Figure 3 displays the diurnal dissolved oxygen curves for the surface waters of all four segments during this testing period. As can be seen in the figure the surface level oxygen levels decrease in all four segments following this rain event. Figures 4 and 5 are diurnal dissolved oxygen curves from the same time period but focus on segments 1 and 3 respectively. These curves show that this drop in oxygen levels was observed at all depths of the canal.

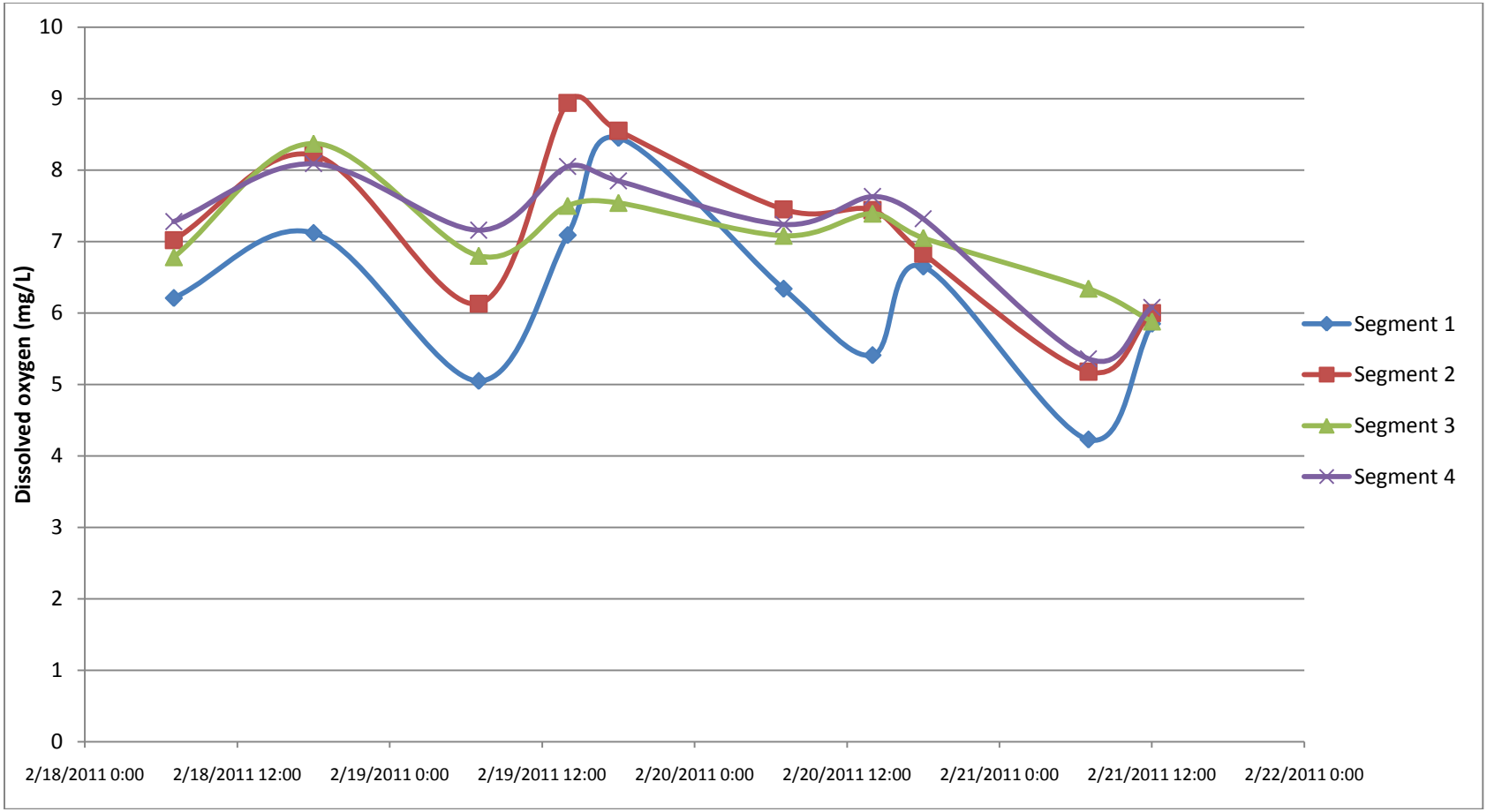

Figure 3. Surface level dissolved oxygen measurements from all four segments from the morning of February 18th through the afternoon on February 22.

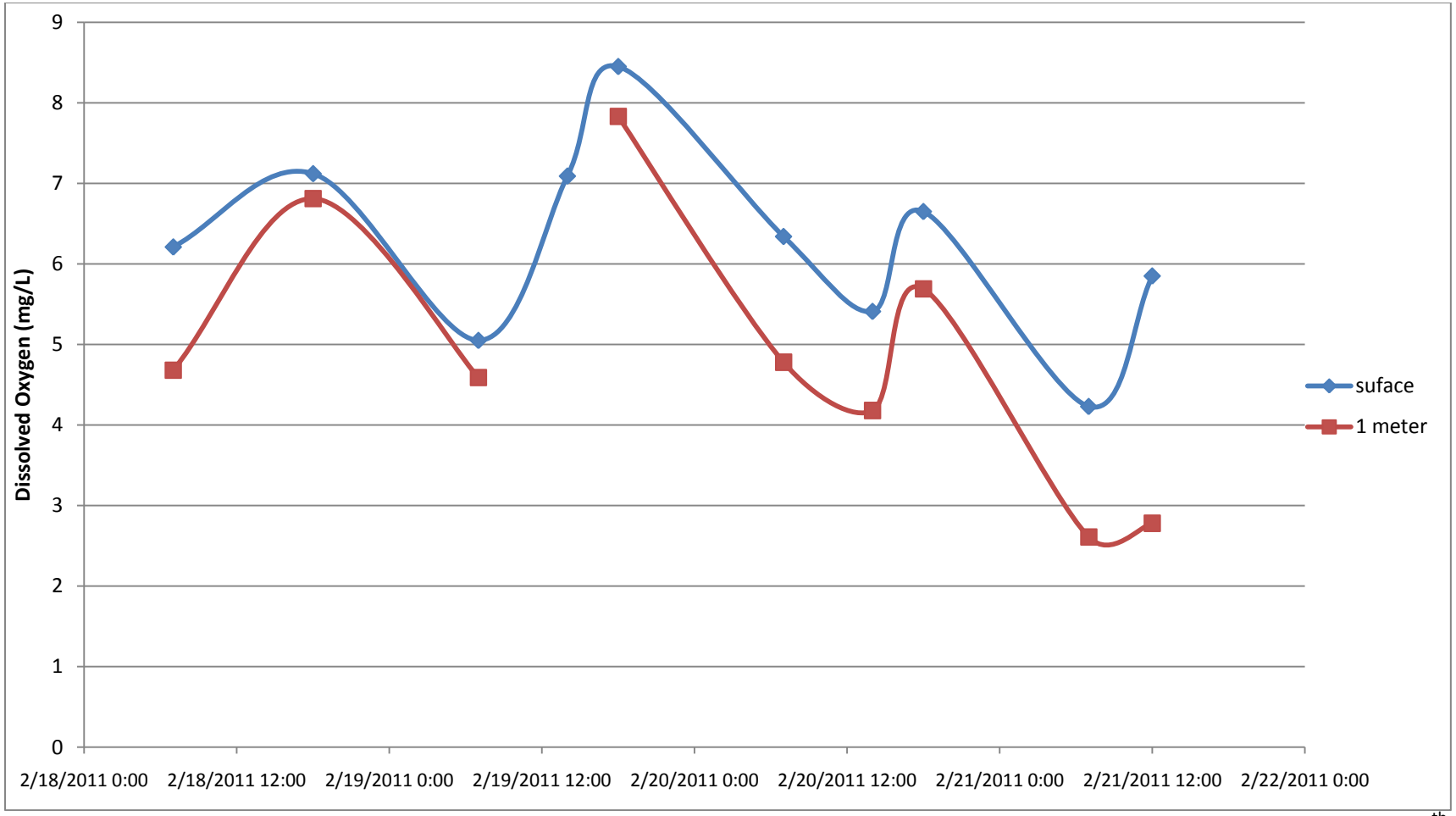

Figure 4. Dissolved oxygen measurements from segment 1 at the surface and a depth of 1 meter from the morning of February 18th through the afternoon on February 22.

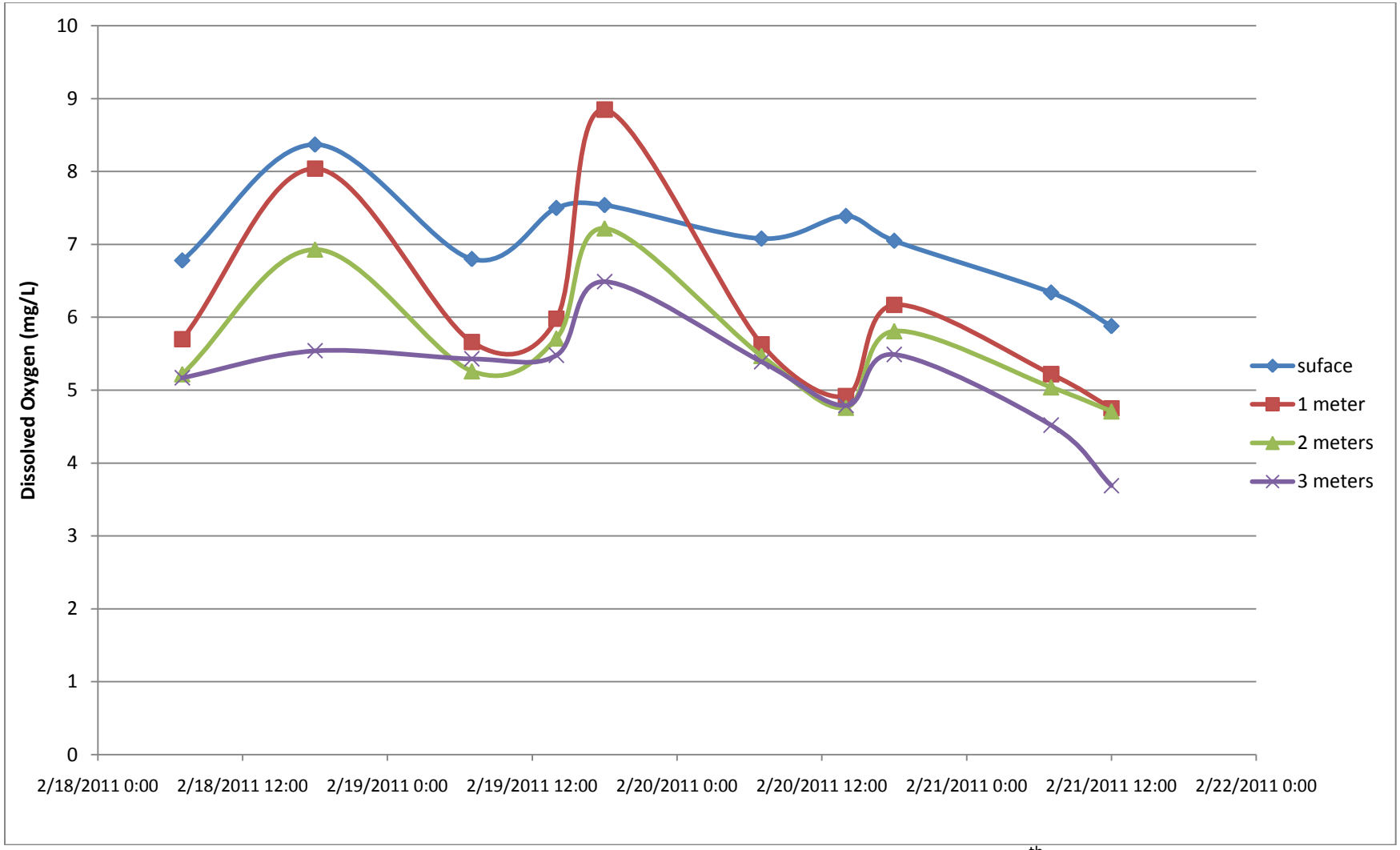

Figure 5. Dissolved oxygen measurements recorded at segment 3 from the morning of February 18th through the afternoon of the 22.

Tidal Effect

There was no clear pattern in differences in dissolved oxygen levels between incoming and outgoing tides. Neither the overall averages nor the dry and wet weather averages revealed any conclusive results. From tables 6-8 it can be seen that although many segments displayed differences in dissolved oxygen levels between ingoing and outgoing tides that the reverse was seen in an almost equal number of other segments or even that same segment at a different time period.

Table 6. Average dissolved oxygen levels (mg liter^{-1}).

Averages	6:00 - 7:30	incoming tide	outgoing tide	12:00 – 14:00	incoming tide	outgoing tide	14:00 – 15:30	incoming tide	outgoing tide	17:00 - 20:00	incoming tide	outgoing tide
Segment 1												
surface	5.51	7.42	5.29	6.6	8.59	5.12	11.97	NA	11.97	7.90	6.87	7.66
half meter	4.83	5.01	4.65	NA	NA	NA	NA	NA	NA	10.51	11.62	9.4
1 meter	4.17	NA	4.17	4.89	7.72	3.48	7.07	NA	7.07	7.32	7.32	7.32
Segment 2												
surface	6.48	6.67	4.78	7.8	8.32	7.02	9.51	8.19	12.15	8.31	7.87	8.75
half meter	5.13	3.44	5.468	8.21	8.21	NA	7.4	7.4	NA	7.74	7.24	7.99
Segment 3												
surface	6.78	6.17	6.84	7.33	7.76	6.26	11.76	NA	11.76	8.60	8.55	8.64
1 meter	5.82	6.13	5.78	6	6.22	5.44	9.61	NA	9.61	8.09	8.01	8.16
2 meters	5.22	4.94	5.25	5.53	5.81	4.83	8.27	NA	8.27	6.90	7.06	6.74
3 meters	5.07	4.52	5.12	5.09	5.48	4.13	6.81	NA	6.81	5.91	5.72	6.10
Segment 4												
surface	6.88	6.72	6.9	7.6	8.3	6.21	9.88	7.63	12.12	8.73	8.74	8.70
1 meter	6.14	6.39	6.1	6.68	7.1	5.83	7.59	5.31	9.87	8.23	8.50	7.94
2 meters	5.49	5.6	5.47	5.94	6.37	5.08	6.58	4.95	8.21	7.24	7.58	6.89
3 meters	6.88	6.72	6.9	7.6	8.3	6.21	9.88	7.63	12.12	8.73	8.74	8.70

Table 7. Dry weather average dissolved oxygen levels (mg liter^{-1})

Dry weather averages	6:00 - 7:30	incoming tide	outgoing tide	12:00 – 14:00	incoming tide	outgoing tide	14:00 – 15:30	incoming tide	outgoing tide	17:00 - 20:00	incoming tide	outgoing tide
Segment 1												
surface	5.92	7.42	5.61	8.59	8.59	NA	11.97	NA	11.97	8.93	9.93	8.18
half meter	4.83	5.01	4.65	NA	NA	NA	NA	NA	NA	10.51	11.62	9.4
1 meter	4.49	NA	4.49	7.72	7.72	NA	7.07	NA	7.07	7.73	8.135	7.32
Segment 2												
surface	6.94	4.78	7.37	9.49	9.49	NA	10.55	8.94	12.15	9.3	9.38	8.76
half meter	5.97	3.44	6.82	8.21	8.21	NA	8.67	8.67	NA	8.16	7.18	8.48
Segment 3												
surface	7.14	6.17	7.34	8.51	8.51	NA	11.76	NA	11.76	9.22	9.47	9.04
1 meter	6.38	6.13	6.424	7.14	7.14	NA	9.61	NA	9.61	8.82	9.03	8.66
2 meters	5.79	4.94	5.96	6.53	6.53	NA	8.27	NA	8.27	7.49	8.19	6.97
3 meters	5.58	4.52	5.79	6.31	6.31	NA	6.81	NA	6.81	6.33	6.44	6.256
Segment 4												
surface	7.49	6.72	7.64	9.04	9.04	NA	12.12	NA	12.12	9.29	9.62	9.04
1 meter	6.58	6.39	6.62	7.84	7.84	NA	9.87	NA	9.87	8.87	9.61	8.31
2 meters	6.09	5.6	6.18	6.95	6.95	NA	8.21	NA	8.21	7.70	8.42	7.16
3 meters	5.83	4.82	6.03	6.425	6.43	NA	7.04	NA	7.04	6.74	7.20	6.39

Table 8. Average wet weather dissolved oxygen levels (mg liter^{-1}).

Wet weather averages	**6:00 - 7:30**	**incoming tide**	**outgoing tide**	**12:00 – 14:00**	**incoming tide**	**outgoing tide**	**14:00 – 15:30**	**incoming tide**	**outgoing tide**	**17:00 – 20:00**	**incoming tide**	**outgoing tide**
Segment 1												
surface	4.90	NA	4.90	5.12	NA	5.12	NA	NA	NA	5.51	5.51	NA
half meter	NA	NA	NA	NA	NA	NA	NA	NA	NA	NA	NA	NA
1 meter	3.70	NA	3.70	3.48	NA	3.48	NA	NA	NA	5.69	5.69	NA
Segment 2												
surface	5.79	NA	5.79	6.68	6	7.02	7.44	7.44	NA	6.01	5.6	6.83
half meter	3.76	NA	3.76	NA	NA	NA	6.13	6.13	NA	6.91	7.29	6.52
Segment 3												
surface	6.23	NA	6.23	6.45	6.64	6.26	NA	NA	NA	7.13	7.18	7.05
1 meter	4.99	NA	4.99	5.14	4.84	5.43	NA	NA	NA	6.38	6.49	6.17
2 meters	4.38	NA	4.38	4.78	4.74	4.83	NA	NA	NA	5.52	5.38	5.81
3 meters	4.29	NA	4.29	4.18	4.24	4.13	NA	NA	NA	4.92	4.63	5.49
Segment 4												
surface	5.98	NA	5.98	6.16	6.08	6.21	7.63	7.63	NA	7.4	7.44	7.32
1 meter	5.46	NA	5.46	5.52	4.91	5.83	5.31	5.31	NA	6.72	6.84	6.47
2 meters	4.59	NA	4.59	4.93	4.64	5.08	4.95	4.95	NA	6.17	6.34	5.83
3 meters	4.37	NA	4.37	4.16	3.77	4.36	5.01	5.01	NA	5.07	5.01	5.2

Chlorophyll

All chlorophyll sampling results can be seen in appendix D. Two distinct patterns of chlorophyll concentrations were observed. During conditions that were more or less dry the chlorophyll levels generally increased from the mouth to the head of the canal. However there were a few occasions when segment 2 was found to have higher chlorophyll concentrations than segment 1 and their dry weather averages were fairly similar as seen in table 9.

Rain events altered the pattern of chlorophyll distribution within the canal with each event having different consequences. It was observed that after small rain events the chlorophyll concentrations would generally dip especially in segment 1. Such events are still included in the dry weather averages listed in table 9 because of the ambiguity in creating a clear definition in dry vs. wet weather during the rainy season around the Ala Wai. There were, however, three days of sampling that are included in table 9 as wet weather sampling. This is because multiple rain events during this period created a large amount of runoff into the canal. The runoff created by these rain events noticeably turned the canal a shade of brown for several days. The chlorophyll samples for these days showed a very different pattern than the dry weather. Segments 2, 3, and 4 all saw large spikes in their average chlorophyll concentrations as can be seen in table 9. Segment 1 actually had a slight dip in its chlorophyll concentration from its dry weather averages. Chlorophyll averages in segments 3 and 4 displayed the greatest increases with values 6.2 and 21.8 times greater than their dry weather averages.

A similar problem to that of dissolved oxygen occurred when trying to view tidal differences in chlorophyll concentrations. It appeared that runoff was a much more important factor than tide in terms of chlorophyll concentration. Because of the difficulty defining wet and dry weather I was unable to accurately remove rain as a variable and therefore unable to accurately compare incoming and outgoing tides. However, it did appear that chlorophyll concentrations were generally slightly higher during outgoing tides.

Table 9. Average chlorophyll concentrations (mg m^{-3}) of the four segments.

Averages	Segment 1	Segment 2	Segment 3	Segment 4
Dry Weather	17.76 ± 10.52 (9)	15.83 ± 13.27 (9)	5.86 ± 1.87 (9)	3.60 ± 0.89 (9)
Wet Weather	14.64 ±7.77 (3)	46.12 ± 41.54 (3)	36.32 ± 28.71 (3)	78.59 ± 83.49 (3)
Total	16.98 ± 9.67 (12)	23.41 ± 25.09 (12)	13.48 ± 18.50 (12)	22.35 ± 49.17 (12)

The spatial variation of the data shows that the chlorophyll concentrations increased in an almost exponential manner. The dry weather averages of segments 3 and 4 were very similar then a sharp increase was observed to segment 2 which had similar chlorophyll levels as segment 1. This can be observed in figure 6 which displays the mean dry weather chlorophyll concentrations measured vs. the distance they were measured from the boat harbor.

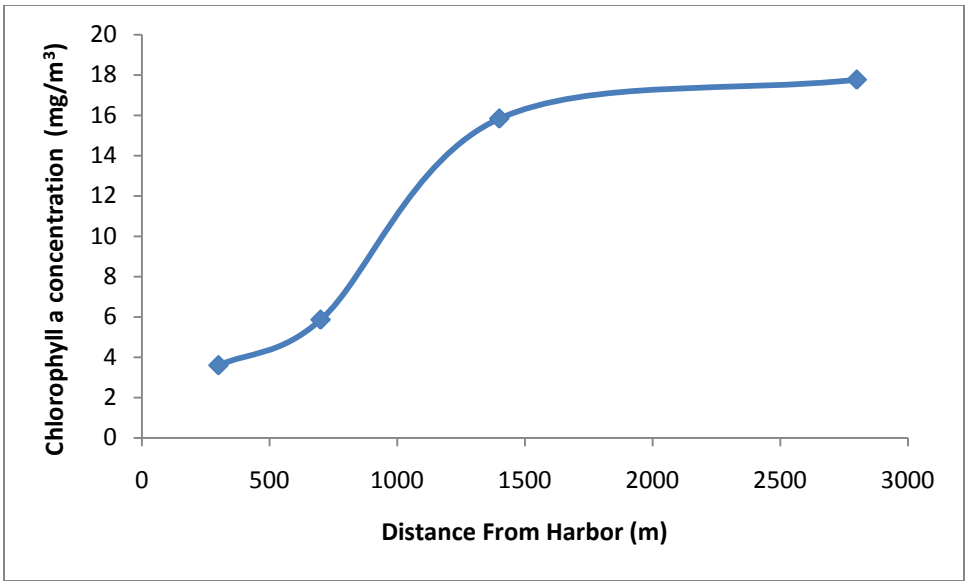

Figure 6. Plot of dry weather chlorophyll *a* concentrations vs. distance from the mouth of the canal.

Field Data Analysis

Chlorophyll

The dry weather chlorophyll concentrations agree with the past studies completed by Harris (1972) and Laws et al. (1994). They both found that chlorophyll concentrations in the canal increased from the head of the canal towards the mouth. Harris (1972) reported slightly larger average values in the range of 9 – 48 mg meter^{-3} while Laws et al. (1994) reported numbers on average 60% smaller than hers. This study's range of 3.60 to 17.76 is in good agreement with those reported by Laws et al. (1994) as they are also roughly 60% less than those reported by Harris (1972).

Increased runoff from rain was shown to have different effects upon the different segments during this study. Runoff showed the capability of lowering the chlorophyll concentrations of all four segments temporarily. This can be explained by the fact that the surface waters were diluted with fresh water containing lower chlorophyll concentrations. Runoff also showed the capability of decreasing the chlorophyll concentration in the first segment while increasing the chlorophyll concentration in the other three segments. An extreme example of this was during the three day period labeled as wet weather in this project. The chlorophyll concentrations in segments 2-4 increased dramatically on the second and third days while the concentrations in segment one actually decreased on the second and third days.

The dry weather chlorophyll *a* concentrations indicate that the Ala Wai Canal is between mesotrophic and eutrophic conditions. The concentrations of the first and second segment suggest these areas are eutrophic while the concentrations of the third

and fourth segments suggest that these areas are in mesotrophic states according to the system given by Wetzel (2001). The wet weather chlorophyll *a* concentrations suggest that during these periods the canal shifts to a much more eutrophic level. All four segments have average concentrations within the eutrophic range with segments 2-4 showing a large increase in chlorophyll *a* production.

Dissolved Oxygen

All four segments showed approximately the same range of ±2 mg liter^{-1} average daily variation for surface level dissolved oxygen levels. The greatest overall variation for both surface water only and surface to bottom waters was observed in segment 1. The level of variation decreased towards the mouth of canal. This finding is in agreement with the past studies completed by Miller (1975) and Laws et al. (1994). It was also towards the head of the canal where the lowest levels of dissolved oxygen occurred. This was also reported by Miller (1975), Laws et al. (1994), and Gonzalez (1971). This study found oxygen levels as low as 1.71 mg liter^{-1} at a depth of 1.5 meters in segment 1 and as low as 2.71 mg liter^{-1} at a depth of a half meter in segment 2. Both of these readings were taken on the same morning two days after a rain event. Despite their greater depth of approximately 4 meters, the oxygen levels in segments 3 and 4 were never observed below 3 mg liter^{-1}. Even the lowest numbers in this study were greater than the low dissolved oxygen readings of 1 mg liter^{-1} and 0.58ppm reported by Gonzalez (1971) and Miller (1975) respectively. This may be because these samples were taken at depths of greater than 3 meters towards the head of the canal. This study was done from land, and no areas that deep were accessible from the shore. It is

therefore likely that at deeper depths towards the head of the canal that dissolved oxygen levels drop even lower than the 1.71 mg liter^{-1} recorded in this study.

Possible reasons for the increased productivity and larger variations in dissolved oxygen levels towards the head of the canal have been investigated by past studies. One possible explanation is the poor circulation and flushing of water found in segment 1. The sill deposited from the Mānoa-Palolo drainage canal has created a stretch of the canal that is less than 1 meter deep in many areas. Gonzalez (1971) concluded that water exchange behind this sill was infrequent and driven by temperature differences. Laws et al. (1994) further concluded that the low dissolved oxygen levels found in these waters may be a exacerbated by the oxygen demand of the sediments which he calculated to be half that of the water column on an areal basis.

Dissolved oxygen levels were also found to be supersaturated on a number of occasions in all four of the segments. This is consistent with data found in previous studies of Miller (1975) and Laws et al. (1994). The highest readings were recorded during the late afternoon and at sunset. These high levels of dissolved oxygen concentration point to the fact that the Ala Wai Canal is a highly productive estuary.

Increased runoff into the canal did appear to have an effect on the oxygen levels within the canal. On a number of occasions the dissolved oxygen levels would dip after a rain event. The largest such dip in oxygen levels occurred after the previously discussed rain event that deposited enough suspended sediment into the canal to noticeably turn the water brown for two days. This study was unable to pinpoint the exact cause of this dip in dissolved oxygen levels after rain. A similar storm was later

studied and is discussed in the chlorophyll section. The chlorophyll data suggested greatly increased phytoplankton concentrations following the storm at least at the surface. It is therefore unlikely that the increased sediment in the canal was entirely responsible for decreasing oxygen production by decreasing bioproductivy. The low levels of oxygen were also first recorded only a few hours after the rain had stopped. This suggests that there was not sufficient time for any type of an algal bloom to occur that would lead to a die off and hypoxia. It is therefore the belief of this author that the increased runoff has an effect on the BOD loading or COD of the canal and that may be a possible cause of the decreased oxygen levels following rainstorms.

C-Value

Diurnal dissolved oxygen data can be used to determine photosynthetic and respiration rates in flowing water bodies (Odum, 1956; Chapra, 1997; Wang et al., 2003). The method used in this paper is the extreme value method (EVM) derived by Wang et al. (2003). This method recognizes three sources and sinks of dissolved oxygen in water. These are air-water exchange, photosynthesis, and respiration. This is a simplified method that does not take into account other factors such as biochemical oxygen demand in its oxygen equations. In the EVM method the variables of photosynthesis and respiration are straightforward and easy to understand. During the day photosynthesis is a source of dissolved oxygen for a water body. Oxygen production due to photosynthesis can be described as a half-sinusoid function with maximum photosynthetic oxygen production occurring at the solar noon (Chapra, 1997). Respiration is a sink that depletes dissolved oxygen levels throughout the day. Because

this reaction is not light-dependent it can be assumed constant throughout the day. The exchange of oxygen between the air-water interface can be both a source and a sink of dissolved oxygen and is regulated by the water's oxygen saturation levels. These saturation levels are a function of both temperature and salinity. When the dissolved oxygen content of a water body is below its saturation levels then oxygen will readily diffuse from the air into the water. However, if the dissolved oxygen content of the water body exceeds its saturation level then this diffusion is reversed and the air becomes a sink for oxygen.

The extreme value method derived by Wang et al. (2003) uses the following equation to describe the change in dissolved oxygen levels of a stream over time:

$$dC/dt = P(t) + k_a(C_s - C) - R \quad (1)$$

where C is the DO concentration (mg liter^{-1}), t is the time (day), C_s is the saturated DO concentration (mg liter^{-1}), k_a is the reaeration rate constant (day^{-1}), P(t) is the photosynthetic rate (mg liter^{-1} day^{-1}), and R is the respiration rate (mg liter^{-1} day^{-1}).

The first step of the extreme value method is to determine the respiration rate using equation 1. Respiration rates are determined from the minimum concentration of dissolved oxygen in a diurnal dissolved oxygen curve. This event occurs before sunrise so the rate of photosynthesis can be assumed to be zero. Also at this point the rate of change of dissolved oxygen can be considered zero so equation 1 can be simplified to:

$$R = k_a(C_{s,min} - C_{min}) = k_aD_{max} \quad (2)$$

where C_{min} is the minimum DO concentration in a diurnal curve (mg liter^{-1}), $C_{s,min}$ is the saturated DO concentration corresponding to the temperature at C_{min} in a diurnal curve (mg liter^{-1}), and D_{max} is the maximum DO deficit (mg liter^{-1}).

To use equation 2 the reaeration rate constant and maximum dissolved oxygen deficits for each segment must be calculated. Chapra (1997) suggests using the O'Connor-Dobbins formula to determine reaeration rates for streams that are 0.30-9.14 meters deep.

$$k_a = 3.93 (U^{0.5}/H^{1.85}) \quad (3)$$

where U is the cross-sectional averaged flow velocity (m/s), and H is the water depth (m)

The cross-sectional averaged flow velocity was determined using the calculated flushing time of 45 hours and the calculated canal volume of 721,618 m^3. These numbers were used in the equation flow (Q) = volume/retention time. Flushing time and retention time are not exactly the same, but this should still provide a rough estimate of the flow within the canal. Using this equation the flow was calculated as 11.14 m^3/s. Using data given by Gonzalez (1971) the average width of the canal was determined to be approximately 68 meters. From the dredging data seen in figure 8 and personal observations the average depth of the canal was estimated to be 2.9 meters. From this the average cross sectional flow velocity was calculated to be 0.056m/s. Using 0.056 for a U value and 2.9 meters as the average depth, k_a was calculated to be 0.130 d^{-1}.

The maximum dissolved oxygen deficits were calculated using the lowest dry weather surface water oxygen data that was collected before sunrise during sampling. These values were 4.12, 4.78, 6.17, and 6.72 mg $liter^{-1}$ for segments 1-4 respectively. During this sampling period an average temperature of roughly 23 degrees Celsius was observed in the surface waters at sunrise. Because the water is brackish a midpoint

between fresh and salt water saturation levels at this temperature was used to determine the oxygen saturation level at this time to be 7.78 mg liter^{-1}. Using equation 2 the respiration rates for segments 1-4 respectively were calculated as 0.48, 0.39, 0.21, and 0.14 (mg liter^{-1} day^{-1}).

The next step was to determine the maximum photosynthetic rate. At the daytime high of dissolved oxygen a peak is reached and similar to the predawn low there is momentarily no change in dissolved oxygen levels. Because of this equation 1 can be simplified at this point to:

$$P(t_{minD}) = R - k_a(C_{s,max} - C_{max}) = R - k_a D_{min} \quad (4)$$

where $P(t_{minD})$ is the photosynthetic rate at the time (t_{minD}) with the minimum DO deficit (mg liter^{-1} day^{-1}), $C_{s,max}$ is the saturated DO concentration corresponding to the temperature at C_{max} in a diurnal curve (mg liter^{-1}), C_{max} is the maximum DO concentration in a diurnal curve (mg liter^{-1}), and D_{min} is the minimum DO deficit (mg liter^{-1}).

The use of this equation requires that the minimum dissolved oxygen deficit be determined for each segment. The daytime highs for dissolved oxygen were 11.97, 12.15, 11.76, and 12.12 (mg liter^{-1}) for segments 1-4 respectively. Temperatures taken in the afternoon averaged approximately 25 degrees Celsius giving a saturation level of 7.50 mg liter^{-1}. This means that all of these oxygen deficits were actually negative meaning they will actually be added to the respiration rate to determine the photosynthetic rate. Using equation 4 the photosynthetic rates of segments 1-4 were calculated as 1.06, 0.99, 0.76, and 0.74 (mg liter^{-1} day^{-1}). It is then desirable to find the maximum rate of photosynthesis for each segment. This is based on the theory that photosynthetic oxygen production can be represented by a half-sinusoid function with

the greatest rate occurring at the solar noon. The maximum rate of photosynthesis can therefore be determined by the equation:

$$P_{\max} = \frac{P(t_{\text{minD}})}{\sin(\pi t_{\text{minD}}/f)} \tag{5}$$

where f is the photoperiod (hours), and t_{minD} can be calculated as $\Delta t + 0.5f$ where Δt is the time shift of the minimum DO deficit from the solar noon (hours).

All of the measurements for maximum DO levels were taken on February 26, 2011. The sunrise was at 6:55 and the sunset at 18:34 giving a photoperiod of 11.65 hours and a solar noon of 12:45. The dissolved oxygen measurements for segments 1-4 respectively were recorded at 14:05, 14:40, 14:20, and 14:30. Using these data the times of minimum DO deficit (t_{minD}) of the four segments were calculated as 7.16, 7.75, 7.41, and 7.58 hours. Using these values the maximum rates of photosynthesis of segments 1-4 respectively were calculated as 1.13, 1.14, 0.84, and 0.83 (mg liter^{-1} day^{-1}).

The respiration and photosynthetic rates alone can give a good description of productivity within a water body. However, the goal of this study was to describe the overall health of the canal using these two rates. Liu (1982) describes a relationship between the maximum rate of photosynthesis, respiration, and the overall health of a water body. A ratio of respiration over the maximum rate of photosynthesis will provide a constant.

$$C = R/P_m \tag{6}$$

The value of this constant can be used to describe the health of the Ala Wai Canal. A general rule is the higher the constant the more productive the stream is.

Where a constant ratio of 0.3 represents a highly productive stream and a ratio close to 0.1 represents a water body of lower productivity. Using equation 6 the constants for segments 1-4 were determined to be 0.42, 0.34, 0.25, and 0.17.

The C-values agree with the chlorophyll data that was obtained for this paper that during dry weather conditions bioproductivity is greatest towards the head of the canal. The high ratios determined for the first two segments suggest that these areas are heavily polluted with excess nutrients which agrees with the past studies of Laws et al. (1994) and Harris (1972). Segment 3 still has a particularly high ratio suggesting that this area of the canal is also facing problems of high bioproductivity. Segment 4 was determined to have the lowest level of productivity of the four segments based on this method.

The C-value calculations were done only for dry weather situations. This is because it was feared that other factors such as possible BOD loading may have affected DO levels after rain events. Also some of the lowest dissolved oxygen levels during wet weather were actually observed during the afternoon. The use of these numbers would be inaccurate as photosynthesis would also be occurring at the moment of maximum DO deficit leading to inaccurate values for respiration. Therefore it is worth noting that the calculated C-values do not take into account conditions immediately following rain. Based on the high productivity observed from chlorophyll data it is assumed the C values would be much greater if wet weather data were also available to be analyzed.

Development of Ala Wai Canal Water Quality Model

A receiving water model that deals with the delivery and transport of nutrients and their biological effect on the canal was created. This section pertains to the initial creation of a nutrient model which will later be used to model nutrient concentrations and changing phytoplankton concentrations throughout the canal. This nutrient model is also used determine if the state's water quality standards are met within the canal.

Several steps were undertaken in the creation of this model. The first was that the loading of nutrients into the canal was broken into two seasons based on the average monthly input of freshwater into the canal.[1] A flushing time was then calculated for each of the two seasons. The transport of nutrients was then modeled based on a series of four CSTRs. The boundaries of the CSTRs were chosen based on changes in salinity and location of major freshwater inputs. The loading and transport of nutrients was assumed to follow the pattern of a step function.[1]

Seasons

The hydraulic properties of the canal were broken into two conditions; the wet season and the dry season. The two seasons were defined from the average amount of freshwater flow entering the canal from nine modeled sources. These data can be seen in table 10. The table represents the monthly averages of total flow entering the canal from 2002 through 2009. From the table it can be seen that the months of October through March have the highest average flows into the canal. The average flow of these six months is 52.1cfs where as the average flow into the canal from April through

[1] Note that the loading data is based on the previously discussed HSPF modeled data. There were nine modeled segments that fed into the canal. Each segment is listed in tables 8 and 10.

September was calculated to be 29.5cfs. Based on these data the wet season was determined to be from October through March, and the dry season determined to be from April through September.

Table 10. Average monthly freshwater inputs into Ala Wai Canal (cfs) 2002-2009

January	February	March	April	May	June
55.8	51.8	61.8	33.0	27.9	34.3
July	August	September	October	November	December
26.0	24.6	31.3	45.2	52.1	45.7

Flushing Time

When modeling an estuary the most important hydraulic parameter is the flushing time. Flushing time is defined as the length of time required to replace the existing fresh water in an estuary at a rate equal to the river discharge. In other words, flushing time represents the average time that a particle spends within the estuary based on its input position. For this study the fraction of freshwater method given in the EPA Water Quality Assessment report of 1977 was used to determine the flushing time of the Ala Wai Canal. The basis of this method is that river flow and runoff are responsible for the freshwater within an estuary. There is a certain volume of freshwater within the estuary, and the flushing time can be approximated by how long it would take the incoming surface water runoff and river discharge to create that volume. One added benefit to this method is that the canal must be divided into segments based on salinity differences. This step ties in with the goal of treating the Ala Wai Canal as a series of completely mixed reactors. The fraction of freshwater method is a six step

method, and the six steps will be shown along with the determination of the two seasons' flushing times for the canal.

Step 1: Graph the salinity profile of the estuary

Because this model deals with long term averages it was important to use a number of different salinity profiles from each season. It was also important that if any past salinity data was used that the data would still accurately represent the canal today. The canal has been dredged multiple times in past few decades, so it had to be verified that this did not affect the mixing characteristics of the canal. The canal was last dredged in 2002, so any salinity data after that should be valid. The salinity data discussed in the field work section was used as a dry season profile. A salinity profile gathered by the Naval Research Laboratory for their 2009 paper "Bacterial Production and Contaminant Mineralization in Sediments of the Ala Wai Canal, Oahu, Hawaii" was used as a wet season profile. This profile was measured in December of 2003 after a rain event, so it coincides with the wet season conditions. The profile can be seen in figure 7.

The dry season data and the data from the Naval Research Laboratory was then analyzed along with past studies to see if there were any major differences between these data and pre-dredging salinity tests. There were no distinct differences observed which made pre-dredging salinity data available for this model. Because more data was desired for a better seasonal average, the data gathered by this study and the Naval Research Laboratory was averaged with data from the 1971 study done by Frank Gonzalez. This study provided ten additional salinity profiles to be averaged with the

recent two. All ten were used to remove any selection bias. Each was divided into its specific season and averaged. Two profiles, collected on April 1st and March 28th were averaged with each season because they fell right on the border of the two seasons.

An average salinity for each segment was then determined for surface water, at a depth of a half meter, and at depths of 1, 2, 3, and 4 meters where segments were that deep. These salinity data can be seen in tables 11 and 12.

Table 11. Average dry season salinity data. All data are given in parts per thousand.

Average Dry Season Salinity						
Segment #	Surface	Half Meter	1 Meter	2 Meters	3 Meters	4 Meters
1	23.77	29.71	32.02	33.20	33.51	-
2	15.71	25.00	30.87	33.12	-	-
3	19.87	26.10	28.85	31.57	33.31	-
4	22.04	27.24	31.97	33.50	33.57	33.65

Table 12. Average wet season salinity data. All data are given in parts per thousand.

Average Wet Season Salinity						
Segment #	Surface	Half Meter	1 Meter	2 Meters	3 Meters	4 Meters
1	24.94	26.62	28.86	32.96	33.40	-
2	17.88	21.42	27.60	32.14	-	-
3	16.38	22.20	26.74	28.60	32.96	-
4	17.90	23.58	30.34	33.42	33.52	33.52

Step 2: Divide the estuary into segments based on the salinity profile

The salinity profile from the Naval Research Laboratory paper was used for this step. The segments derived from this salinity profile match well with major freshwater inputs into the canal. This is important because the canal will be modeled as a series of CSTRs. One characteristic of a CSTR is that it is assumed to be perfectly mixed. This best holds true if the inputs into the segment are in the back forcing the water to travel

throughout the entire segment. The segments in this salinity profile are good because the two major inflows into the canal (Mānoa-Palolo and Makiki) are positioned at the back of segments 2 and 4 respectively in the figure below.

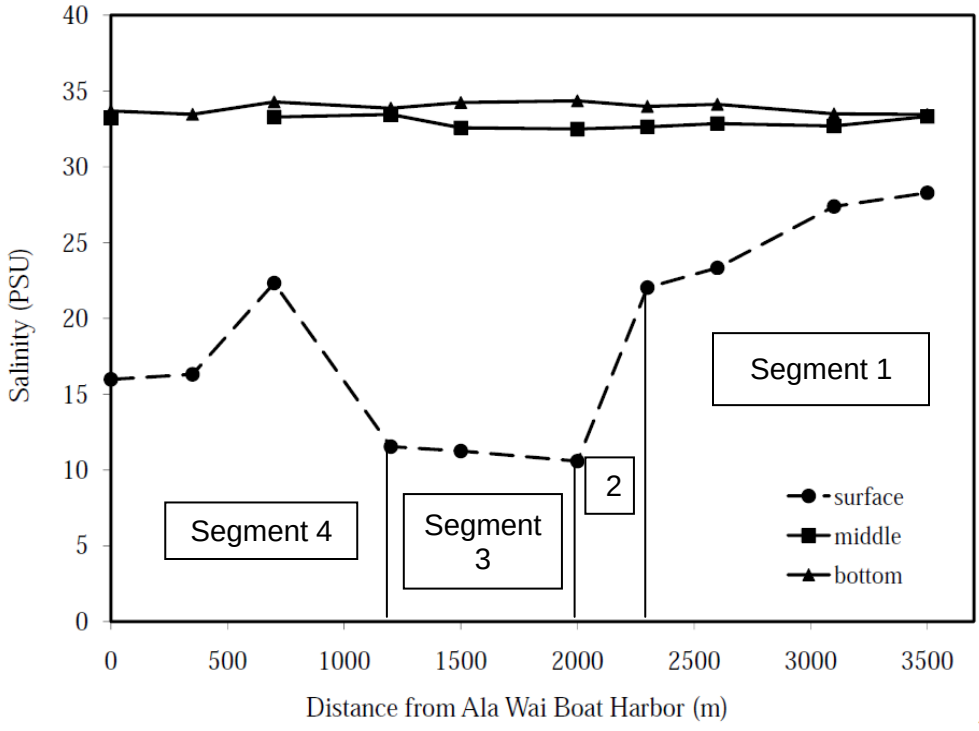

48

Figure 7. Wet Season salinity profile and segment boundaries of the Ala Wai Canal

Step 3: Calculate each segment's fraction of freshwater by:

$$f_i = \frac{S_s - S_i}{S_s}$$

f_i = fraction of freshwater in segment "i"
S_s = salinity of sea water
S_i = mean salinity for segment "i"

The first step in this method was to determine the mean salinity for each of the four segments for each of the two seasons. Using the information in tables 11 and 12 an average salinity was calculated for all segments. These average salinities can be seen in tables 13 and 14.

The salinity of Mamala Bay was used as the salinity of sea water. This should be accurate because Mamala Bay is the salt water source of the Ala Wai. The mean salinity of Mamala Bay is roughly 34.55 parts per thousand (Lau & Mink, 2006). From these data the fraction of freshwater for each segment was calculated. The fraction of freshwater data can be seen in tables 13 and 14.

Table 13. Average dry season salinity and fraction of freshwater data for the four segments.

Segment Number	Average Salinity	Fraction of Freshwater
1	31.49	0.0885
2	24.14	0.3012
3	29.53	0.1452
4	31.74	0.0812

Table 14. Average wet season salinity and fraction of freshwater data for the four segments.

Segment Number	Average Salinity	Fraction of Freshwater
1	30.30	0.1230
2	22.75	0.3416
3	27.24	0.2116
4	30.70	0.1114

Step 4: Calculate the quantity of fresh water in each segment by:

$$W_i = f_i \times \text{low tide volume of segment}$$

W_i = quantity of freshwater in segment "i"

The low tide volume is suggested by the EPA because it represents a worst case scenario for flushing time. However, because this study is interested in a long term average for flushing time (wet and dry seasons) the mean volume of each segment was used instead of the low tide volume. The depth of each segment was estimated using the planned post 2002 dredging depth of the canal shown in figure 8. However, when

collecting dry season salinity data it was obvious that the area directly below the Mānoa-Palolo drainage canal had undergone significant sedimentation since dredging. In many areas it is not much more than a meter deep. This was taken into account as well when estimating the depth for that segment. The depths of each segment were then multiplied by the surface area data given by Noda and Associates in their feasibility report to obtain a volume for each segment. The volume of each segment and their corresponding W_i value for each season can be seen in table 15.

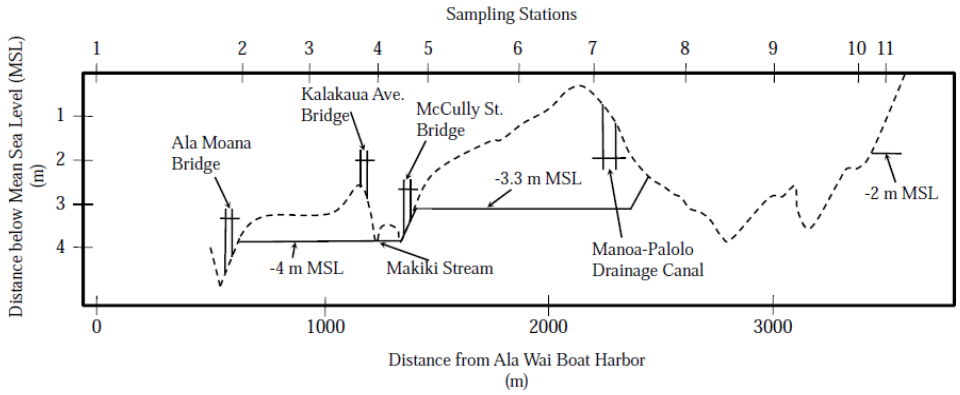

Figure 8. Proposed dredging depths of Ala Wai Canal 2002

Table 15. Volume and corresponding quantity of freshwater for each of the four segments

Segment Number	Volume (m^3)	Dry Season Quantity of Freshwater (m^3)	Wet Season Quantity of Freshwater (m^3)
1	260,070	23018	32000
2	58,740	17695	20067
3	172,216	25006	36440
4	230,592	18735	25679

Step 5: Calculate the flushing time for each segment by:

$$T_i = W_i/R$$

T_i = segment flushing time
R = total river discharge over one tidal cycle

The fifth step of the process was to calculate the flushing time of each segment. To do this the R-value of each segment had to be determined. To do this all freshwater flows into each segment had to be determined. The average monthly flows of each input are summarized below in tables 16 and 18. For example the dry season flows into segment one based on the previously created HSPF model are the golf course, Waikiki 1, and the zoo. Combined these three inputs had an average flow of 11.3 cubic feet per second. To determine the R-value this had to be converted to cubic meters per tidal cycle. The formula for this is as follows:

$$11.3\text{cfs} \times \frac{0.0283\text{cubic meters}}{1.0\text{ cubic foot}} \times \frac{3600\text{ seconds}}{\text{hour}} \times 12.4\text{ hours/tidal cycle}$$

For segment one the R-value was calculated to be 14,275 cubic meters of freshwater per tidal cycle. Each additional segment's R-value was calculated similarly, but with one additional step. Each downstream segment's R-value had to be added to all upstream segments' R-values. This step assumes that an equal amount of freshwater that enters a segment over one tidal cycle is therefore passed onto the next segment during the following tidal cycle. For example the R-value for segment 2 would be based on Mānoa-Palolo and Waikiki 2 only if this step were not included. However, the freshwater that enters from segment 1 must also be accounted for, and therefore the total R-value for segment 2 represents flows from the golf course, Waikiki 1, the zoo, Mānoa-Palolo, and Waikiki 2. The average freshwater inputs into the canal, calculated R-values, and flushing times of each segment are given in the tables below.

Table 16. Average dry season flows (cfs) from all 9 HSPF inputs into canal

Dry Season Average Freshwater Inputs (cfs)				
Mānoa-Palolo	Golf Course	Zoo	Makiki	Ala Wai-Park
10.14	7.96	0.94	4.38	0.72
Waikiki 1	Waikiki 2	Waikiki 3	Waikiki 4	-
2.40	0.48	0.57	0.94	-

Table 17. Calculation of dry season flushing times for each segment

Section	Freshwater Inputs	R-Value (m^3/tidal cycle)	Flushing Time (hours)
1	Golf, Waikiki 1, Zoo	14,275	20.00
2	Man-Pal, Waikiki 2	27,691	7.92
3	Middle, Waikiki 3	29,320	10.58
4	Makiki, Waikiki 4	36,040	6.45

Table 18. Average wet season flows (cfs) from all 9 HSPF inputs into canal

Wet Season Average Freshwater Inputs (cfs)				
Mānoa-Palolo	Golf Course	Zoo	Makiki	Ala Wai-Park
19.07	9.20	1.19	11.40	1.43
Waikiki 1	Waikiki 2	Waikiki 3	Waikiki 4	-
2.79	0.98	1.028	1.77	-

Table 19. Calculation of wet season flushing times for each segment

Section	Freshwater Inputs	R-Value (m^3/tidal cycle)	Flushing Time (hours)
1	Golf, Waikiki 1, Zoo	16,650	23.83
2	Man-Pal, Waikiki 2	41,979	5.93
3	Middle, Waikiki 3	45,086	10.02
4	Makiki, Waikiki 4	71,426	4.45

Step 6: Calculate flushing time of the estuary

The final step was simply the addition of each individual segment's flushing time to determine the flushing time for the estuary. The sum of the four individual flushing times was 45.0 hours for the dry season and 44.2 hours for the wet season. These two flushing times were used as the hydraulic parameters of all nutrient and biological modeling discussed in the next chapter.

The flushing times for each season were calculated to be very similar. It may be that despite big differences in freshwater input the overall flow within the canal remains dominated by ocean current. It may also just be a coincidence that these two flushing times were so similar based on the data that was used. However, nine years of flow data and twelve salinity profiles were used suggesting that if they are not the same then the two flushing times should be very similar.

The 44/5 hour flushing times also agree with the dye test run by Noda and Associates that was used to determine the mean residence time of the canal. Their test indicated that the mean residence time of the dye within the canal was between 40-60 hours (E.K. Noda and Associates Inc., 1992). The dye represents a conservative particle of pollutant that enters the canal, so in the absence of any other reactions the mean residence time of a particle within the canal should be approximately 40-60 hours. Mean residence time is not exactly the same as flushing time, but this does show that the calculated 45 hour flushing time is in approximate agreement with other methods used.

Despite their closeness, the two calculated flushing times will still be used for the receiving water model. This is because although each season has a similar overall flushing time, the flushing times of each of their segments vary somewhat. Therefore each season's flushing time will be included in the modeling of nitrogen and phosphorus concentrations.

CSTR Model

The next stage of this model was to model the nitrogen and orthophosphate within the canal. As previously discussed the Ala Wai Canal was divided into four segments based on salinity and location of freshwater inputs. Each of these four segments will be assumed to behave as the laws of a CSTR dictate. That is that once a load has been introduced into the reactor it is completely mixed throughout giving the entire segment an equal initial concentration of that substance. The simple written mass balance equation for a CSTR is as follows:

rate of change of mass accumulation = loading – outflow – reaction – settling

The rate of change of mass accumulation is the final outcome of the reactor that is most important when dealing with loading within an estuary. This equation explains the processes by which nutrients might accumulate within the canal. Ideally there would be no accumulation within the canal, and the loading would be completely offset by the outflow, reaction, or settling of the nutrient. However, this is not the case, and therefore the rate at which accumulation takes place within the canal must be calculated. Accumulation ultimately represents the change of mass in the system over time as represented by the equations below:

$$accumulation = \frac{\Delta \mathrm{M}}{\Delta \mathrm{t}}$$

ΔM = change in mass
Δt = change in time

The concentration of the substance is related to mass by the following equation that states that concentration is equal to mass/volume.

$$c = \frac{\mathrm{M}}{\mathrm{V}}$$

Therefore the mass of the pollutant will be equal to the concentration of the pollutant multiplied by the volume of water within that segment:

$$\mathrm{M} = \mathrm{Vc}$$

Assuming that the volume of the canal is constant then the overall equation for accumulation equation can be rewritten as follows:

$$accumulation = \mathrm{V}\frac{\mathrm{dc}}{\mathrm{dt}}$$

This equation states that if the volume of the estuary is assumed constant then accumulation is simply a result of a change in concentration over a change in time. The volume of an estuary is in fact not constant, but in this model long term averages are used and the volume of the canal can be deemed constant.

The next parameter in the equation for accumulation is the input parameter known as loading. Loading is the adding of pollutants into the system. For these models the loading represents the total nitrogen or orthophosphate added to the Ala Wai Canal from the nine inputs due to runoff. Because these models represent series of continuously stirred tank reactors it does not matter where the loading occurs within each segment. As soon as the load is introduced into the segment it is assumed to be perfectly mixed throughout. However, for more accurate results the canal was segmented so that the inputs are towards the back of each segment. The equation for loading is as follows:

$$\text{Loading} = \mathrm{W}(t)$$

Where W(t) is the rate of mass loading that is a function of time. The mass loading into the canal can easily be determined by multiplying the concentration of pollutant flowing into a segment by the total volume of water flowing into that segment.

The next parameter of the equation is the loss of pollutant through the process of outflow. In this case it is the movement from one segment to the next and ultimately out of the mouth of the canal and into Mamala Bay. In most situations this is proportional to the flow rate within the reactor divided by the total volume of the reactor. However, because this is an estuary this outflow parameter will be solely dependent upon the previously discussed flushing times.

The next parameter of the equation is the reaction rate. This would occur as a loss from the system. Nitrogen and Phosphorus both react with microorganisms by providing them with the necessary nutrients for growth. It is desired that these nutrient inputs be lowered in the canal to stop excessive growth caused by these reactions. Because of this these reactions will not be considered as losses for the comparison to the state's water quality standards and TMDL limits because the goal is to predict how much of these nutrients are available for these reactions.

The final parameter of the equation is settling rate. This would also occur as a loss from the system, but again with a negative impact. Sedimentation is a big problem in the canal which forces the city to dredge the canal every decade or so. The effects of this process were observed when salinity data was gathered for this report. The area at the outfall of Mānoa-Palolo was nearly two meters shallower than what it was supposedly dredged to eight years ago. Settling would result in a loss of

orthophosphate from the water column. Unfortunately, there is no available data on the specific settling rates that occur at various stages within the canal. Therefore this reaction cannot accurately be included in this model. Thus by removing these final two parameters the simplified equation states that

Accumulation = Loading – Outflow

That represents the simple equation to determine accumulation. The model discussed in this project uses this basic equation to determine nutrient concentrations in the canal based on a process of step loading. A step loading model models a situation that is similar to an on/off switch. The system starts with a loading equal to zero. At a time t = 0 the system is turned on and immediately the loading is raised to a new steady state amount. The concentration of the pollutant within the system then asymptomatically increases towards its steady state concentration. The equation for the new concentration within the system based on this steady state loading is as follows:

$$c = \frac{W}{\lambda V}\left(1 - e^{-\lambda t}\right)$$

where c is equal to the new concentration, W is equal to the new steady state loading, V is the volume of the system, t is the time, and λ is the inverse of the system's retention time (flushing time for an estuary).

After 3-5 flushing times the model will reach a near steady state equilibrium. Once this phase has been reached the long term average concentration within the canal can be viewed. The steady state concentration can be determined by using a simplified equation that states:

$$\overline{c} = \frac{W}{\lambda V}$$

The use of the step loading model will have two benefits for this model. The first benefit is that much of the pollutants are added to the canal occur during a storm event. This will be modeled using an increase in step loading in the next chapter of this report. The step loading function will make visible how the nutrient concentrations change over time as a result of an increased loading rate. The other benefit of using the step loading model is that it ultimately will determine the steady state concentration of the pollutants within the canal and the four segments for each of the two seasons. This is the number that is of most concern for water quality standards and TMDL comparisons because it looks at the long term averages.

Modeling Analysis

Nitrogen Model

The first step to creating the seasonal nitrogen model was to determine the average loading into the canal for each of the nine inputs and in turn each of the four segments. To do this the average hourly load of each input was determined by using the previously discussed data from January 2002 through December of 2009. The average load from the nine inputs into each of the four segments for the two seasons is listed in the table below.

Table 20. Seasonal loading of nitrogen (grams/hour) into each segment

Dry Season		Wet Season	
Segment #	Loading (g/hr)	Segment #	Loading (g/hr)
1	534	1	569
2	1535	2	2505
3	353	3	503
4	507	4	829

There is also a background level of total nitrogen added into these calculations. The background level of nitrogen represents the concentration of nitrogen in the sea water that enters into the canal. This is independent of the loading from runoff. The average level of nitrogen and ammonium in Mamala Bay was taken from the book Hydrology of the Hawaiian Islands by Stephen Lau. Table 8.3 in the book provides mean levels of nitrates and ammonium present within the bay as 0.42 and 0.56 µg/L respectively. Together these represent approximately 1 µg/L as the average background level which will be used in the model. The average concentrations of total nitrogen within the canal for the wet and dry seasons can be seen in figures 9 and 10 respectively.

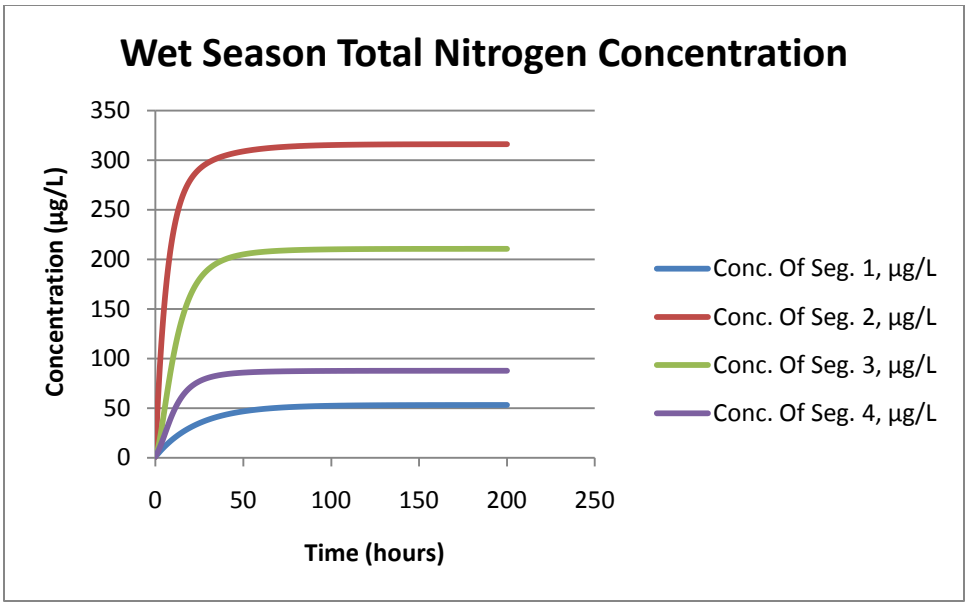

Figure 9. Total nitrogen concentrations (µg/L) within the Ala Wai Canal for the wet season.

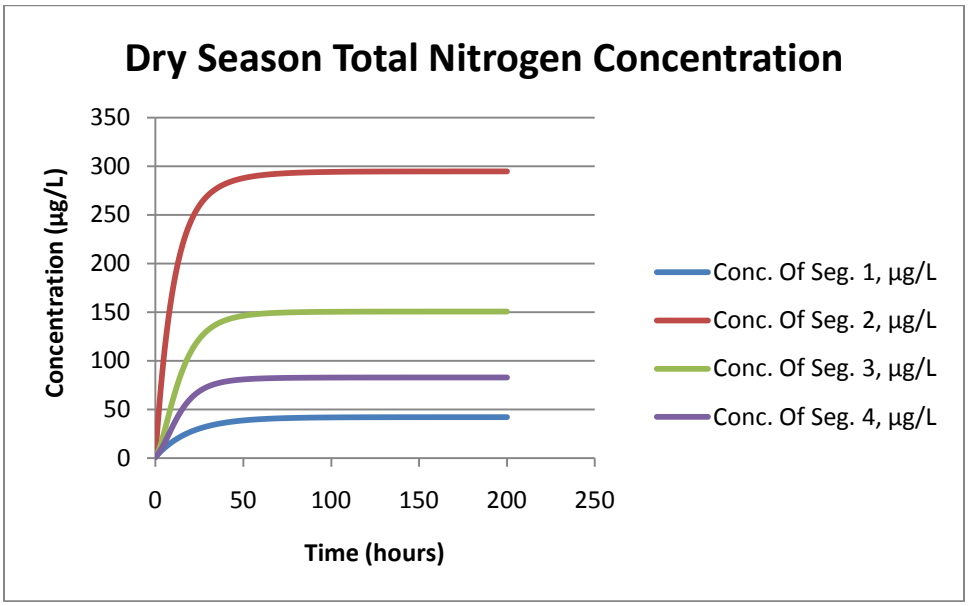

Figure 10. Total nitrogen concentrations (µg/L) within the Ala Wai Canal for the dry season.

The highest concentration of nitrogen is seen in segment 2 for both seasons. The steady state concentrations of the four segments are 53, 316, 211, and 88µg/L for the wet season, and 42, 295, 151, and 83µg/L for the dry season. From these averages

it can be seen that the background level of nitrogen does not factor much in the average concentration within the canal. The total nitrogen concentration within the canal is therefore almost entirely the result of runoff.

Using the segment concentrations and their corresponding volumes the seasonal averages of total nitrogen concentration can be determined for the entire canal. The average concentration for the wet season is 123µg/L, and the average concentration for the dry season is 102µg/L. The modeled averages for both seasons fall below the state's water quality standard for the canal which is 200µg/L. However, areas within the canal such as the second segment for both seasons and the third segment for the wet season are still above the 200 µg/L goal.

Orthophosphate Model

Orthophosphate concentrations within the canal were modeled using the same parameters as nitrogen. However, no background phosphate level was included in this model. The marine waters around the canal do contain phosphorus, but no reliable data was found that contained the concentration of orthophosphate. The average phosphate concentration within the bay was found to be approximately 4 µg/L, but it is unknown what percent of this is orthophosphate. The modeled orthophosphate concentrations can be seen in figures 11 and 12.

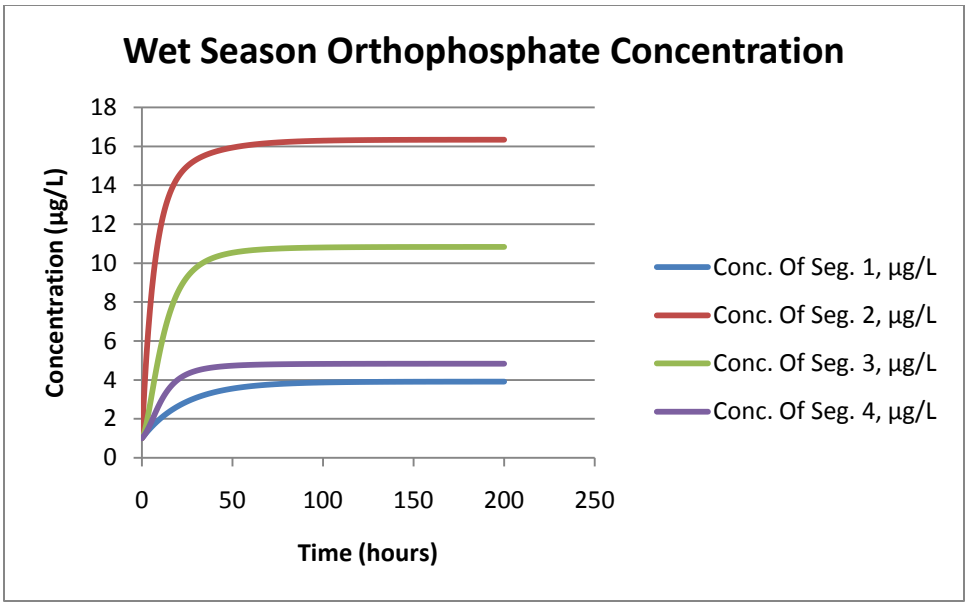

Figure 11. Average wet season orthophosphate concentrations (µg/L)

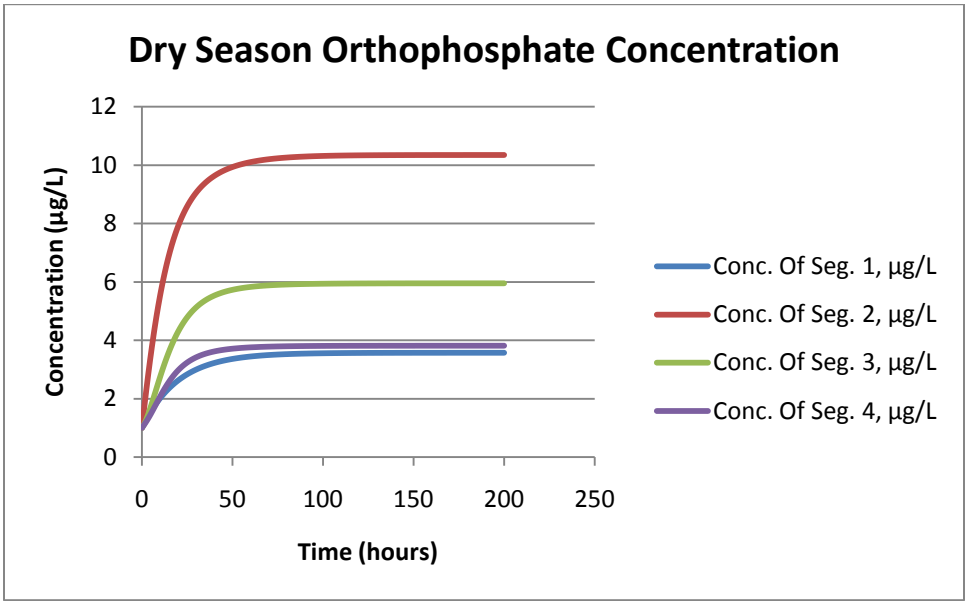

Figure 12. Average dry season orthophosphate concentrations (µg/L)

From the graphs it can be seen that even if a background concentration was determined that the orthophosphate levels are much lower than the total nitrogen concentrations within the canal. Although this is just a portion of the phosphorus in the

canal, it is the most important portion in terms of biological growth. Orthophosphates are the phosphates that are used for plant growth.

The steady state segment concentrations of the four segments were calculated to be 3.9, 16.3, 10.8, and 4.8µg/L respectively for the wet season, and 3.6, 10.3, 6.0, and 3.8µg/L respectively for the dry season. Using these segment averages the seasonal averages for the canal were calculated for orthophosphate concentrations. The average wet season concentration within the canal was calculated to be 6.8µg/L and the average dry season concentration 4.8µg/L. There are no water quality standards that dictate the acceptable levels of orthophosphate in a water body. As a point of reference, the water quality standard for total phosphorus is 25µg/L for the Ala Wai Canal.

Dry and Storm Weather:

The wet and dry seasonal averages are useful in determining if the long term pollutant concentrations meet the water quality standards of the canal. However these are long term averages that incorporate both dry weather and storm events. Here two more conditions are briefly discussed. Dry and storm weather conditions are meant to represent short term conditions of either extremely low levels of loading that would occur during a prolonged period of no rain, or extremely high levels of loading that would occur directly following a storm event. The flushing times of the seasonal averages were used and only the loading levels were changed. One month was chosen to represent each of the conditions. May of 2009 was the month that was calculated to have the lowest levels of nutrient input, and March of 2006 was calculated to be the month of highest nutrient input. These months were used to determine dry and storm

weather conditions. The average hourly loading rates for these two months can be seen in tables 21 and 22.

Table 21. Hourly loading rates for dry weather determined from May of 2009.

Location	NO3 (lbs/hour)	TAM (lbs/hour)	NO2 (lbs/hour)	PO4 (lbs/hour)
Mānoa-Palolo	0.5	0.073	0	0.005
Makiki	0.452	0.115	0.00083	0.0205
Middle	0.352	0.0459	0.00046	0.0176
Zoo	0.033	0.0065	0	0.00208
Golf	0.159	0.0288	0	0.00884
Waikiki 1	0.0364	0.0072	0	0.00225
Waikiki 2	0.0189	0.0036	0	0.00111
Waikiki 3	0.0812	0.0105	0	0.00506
Waikiki 4	0.146	0.0197	0	0.00994

Table 22. Hourly loading rates for storm weather determined from March of 2006.

Location	NO3 (lbs/hour)	TAM (lbs/hour)	NO2 (lbs/hour)	PO4 (lbs/hour)
Mānoa-Palolo	11.4	3.57	0	1.94
Makiki	2.6	1.1	0.0087	0.0823
Middle	2.22	0.081	0.0006	0.0601
Zoo	0.203	0.019	0	0.0154
Golf	1.13	0.104	0	0.0706
Waikiki 1	0.223	0.021	0	0.0169
Waikiki 2	0.126	0.012	0	0.0086
Waikiki 3	0.148	0.014	0	0.0101
Waikiki 4	0.257	0.025	0	0.0197

Using the above loading rates the average nutrient concentrations for each segment were calculated. The calculated nutrient concentrations for each segment during each weather pattern can be seen in table 23. From the table large discrepancies can be seen in the nutrient concentrations within the canal between rain events and periods of no rain. For example the average nitrogen concentration is nearly one and a half times the allowable level of the TMDL standards during the storm period. However, the concentration is less than 15% of the limit when no surface runoff is occurring from rainwater.

Table 23. Average concentrations (µg liter^{-1}) of total nitrogen and orthophosphate during periods of dry weather and storm events.

Condition	Segment 1	Segment 2	Segment 3	Segment 4	Total Average
Total Nitrogen (Dry)	10.5	56.8	39.0	27.5	26.5
Total Nitrogen (Wet)	71.8	782.9	513.7	209.0	279.0
Orthophosphate (Dry)	1.5	2.2	2.2	1.9	1.85
Orthophosphate (Wet)	5.3	96.4	57.4	20.9	30.1

TMDL Limits

In 2002 the state of Hawai‘i changed the format of its TMDL standards. The limits of the TMDL state the average daily mass loads which can be present in the Ala Wai Canal without exceeding the applicable water quality standards. To compare the data from this study to the TMDL limits the nutrient load that travels through each segment per day had to be calculated. Because this study only contains orthophosphate data and not total phosphorus the TMDL limits were only examined for total nitrogen. The current limit set by the TMDL standards for total nitrogen is 25 kg/day.

Because the fraction of freshwater method was used to calculate flushing time, the freshwater volume of each segment was used to calculate the mass of total nitrogen that flows through each segment per day. The first step in calculating this kg/day was to determine the concentration of nitrogen in the freshwater. For this step it was assumed that nitrogen entering through freshwater runoff did not mix with the seawater and vice versa. This means that the background concentration of 1µg/l was subtracted from each season’s average concentration. This freshwater concentration was calculated through the following equation:

{(total concentration – background concentration)/fraction of freshwater} x 1000

The 1000 in the equation was used to convert µg/l to µg/m^3. This equation gave the concentration of nitrogen in the freshwater only. The next step was to determine the volume of water that flowed through each segment per day. To do this the previously determined R value for each segment was used. Because the R value is per a 12.4 hour tidal cycle this value was multiplied by 1.935 to convert to the freshwater flow per day. The volume of freshwater that flowed through each segment per day was then multiplied by the freshwater concentration. This was then multiplied by 10^{-9} to convert from micrograms to kilograms. The calculated loads per day for the wet and the dry seasons can be seen in the tables below.

Table 24. Calculation of wet season total nitrogen flow based on TMDL criteria.

segment #	concentration minus background µg/l	concentration of fresh water only µg/m^3	volume of water (m^3/day)	kg/day
segment 1	52	422800	32226	13.6
segment 2	315	922200	81249	74.9
segment 3	210	992500	87263	86.6
segment 4	87	780900	138243	108.0

Table 25. Calculation of dry season total nitrogen flow based on TMDL criteria.

segment #	concentration minus background µg/l	concentration of fresh water only µg/m^3	volume of water (m^3/day)	kg/day
segment 1	41	463300	27629	12.8
segment 2	294	976100	53595	52.3
segment 3	150	1033000	56748	58.6
segment 4	82	1009900	69754	70.4

As can be seen in tables 24 and 25 the current TMDL limits of 25 kg/day are exceeded for total nitrogen in segments 2-4 for both the wet and dry seasons. It was not possible to do this calculation for the previously discussed wet and dry weather patterns. This is because there were no salinity profiles for these conditions to calculate fraction of freshwater data for each segment. Also different freshwater flow numbers

would need to be calculated. As seen in tables 24 and 25 the calculated freshwater flows for each season are very different unlike the similarity in the closeness of the two flushing times. It would therefore be an incorrect assumption to assume that dry or rainy conditions would show the same freshwater flows as their seasonal averages.

Nutrient Model Discussion

The goal of this model was to give a basic understanding of the concentrations of nutrients within the Ala Wai Canal. From the model it is clear that neither the load nor the concentrations of these pollutants are spread evenly throughout the canal. The majority of the loading of nitrogen and phosphorus occurs via the Mānoa-Palolo drainage canal and Makiki Stream. As such the concentrations of these pollutants within the Ala Wai respond accordingly. The area just below the Mānoa-Palolo Drainage Canal has been shown to incur the greatest concentrations of these pollutants. That is because it has a slightly higher loading rate than Makiki Stream and because the area of the canal below Makiki Stream is deeper and better flushed with seawater.

Using the steps of this model the steady state averages of nitrogen and orthophosphate, were also calculated. The seasonal averages of total nitrogen were below the state's water quality standard's limits for the Ala Wai. However, nitrogen concentrations in segments 2 and 3 during the wet season and segment 2 during the dry season violated the 200µg/l standard.

A rainstorm was also modeled using loading data from March of 2006. It is important to note that the state water quality standards for the canal also include standards for these high loading periods. The standards for the canal state that the

total nitrogen concentration should not exceed 350µg/l more than 10% of the time or 500µg/l more than 2% of the time. Overall the modeled total nitrogen concentration of 279µg/l falls below both of these standards. However, the modeled storm concentrations in segments 2 and 3 both exceed 500µg/l.

The state's current TMDL limits were also modeled to be exceeded for total nitrogen. The limit of 25kg/day for total nitrogen was exceeded for both the dry and wet seasons in segments 2-4. There are a few possible explanations as to why this value was exceeded more often than the desired limits set by the state's water quality standards. The overall major difference is the constraints of the TMDL method. The TMDL standard all ready assumes a high level of background nitrogen inputs from the incoming seawater. The lower levels assumed in the concentration calculations were therefore not able to be used. Also the TMDL limits were based on a canal volume calculated in the early 1990's. The volume used for this paper's water quality standards is based on a greater calculated volume from dredging that occurred in 2002.

Both methods are in agreement that there is a problem with excess total nitrogen within certain areas of the canal. Segment 2 contained the highest concentration of nitrogen of the four segments. This is partially because the largest modeled contributor of total nitrogen to the canal, Mānoa-Palolo Drainage Canal, feeds directly into segment 2. For all segments of the canal to meet both the TMDL limits and water quality standards, nitrogen loading through this input must be reduced.

Chlorophyll Model

The goal of this section is to show how the previously created water quality model can be used to show the biological response to an increase in nutrient concentration within the canal. The previously discussed field data for chlorophyll *a* concentrations was the basis for this model. A storm condition was modeled to give varying nutrient concentrations throughout the canal. The model incorporated growth and decay of phytoplankton to show how these microorganisms' concentrations would change given the varying environmental factors.

The first step of this model was to determine the potential growth of phytoplankton. Phytoplankton growth is based largely on three parameters; temperature, light availability, and available nutrients. A growth rate model that contains these three parameters was chosen from the literature (Chapra, 1997).

$$k_g = k_{g,20}1.066^{T-20}\left[\frac{2.718f}{keH}\left(e^{-\alpha_1} - e^{-\alpha_0}\right)\right] \min\left(\frac{n}{ksn+n}, \frac{p}{ksp+p}\right)$$

Where k_g is the phytoplankton growth rate, $k_{g,20}$ is the phytoplankton growth rate at 20°C, f is the photoperiod (fraction of the day receiving sunlight), k_e is the extinction coefficient (m^{-1}), H is the chosen depth (m), α_1 and α_0 are factors of available sunlight that will be explained later, n and p are available nitrogen and phosphorus concentrations respectively, and k_{sn} and k_{sp} are the half saturation constants for nitrogen and phosphorus respectively.

The first part of the growth model is the temperature dependent growth rate. K_g is the growth rate of phytoplankton that would normally occur at 20 degrees Celsius. Based on the literature an average growth rate of 2.0 $days^{-1}$ was chosen (Chapra, 1997; Zison et al., 1979). The average temperature of the canal was observed to be approximately 25°C.

The second part of the growth equation is the limitation that light has upon growth. An average photoperiod of 12 hours was chosen with a resulting f value of 0.5. The average extinction coefficient in the Ala Wai was measured as $1.13 m^{-1}$ by Laws et al. (1994). A depth of 1 meter was chosen as the depth to simulate chlorophyll growth in this model. The two alpha terms were calculated using the following equations:

$$\alpha_0 = (I_a/I_s)e^{-keH1} \qquad \alpha_1 = (I_a/I_s)e^{-keH2}$$

The I_a term represents the incident light, which is 462 langleys day^{-1} for an average day in Honolulu. The I_s term represents the optimum light level for phytoplankton growth and a value of 300 ly d^{-1} was chosen based on the literature (Chapra, 1997). H_1 and H_2 represent depths of 0 and 1 meters respectively in this model.

The final part of the growth model is the nutrient limitation on growth. Typically growth is either limited by available levels of nitrogen or phosphorus. A molar ratio of 16:1 nitrogen to phosphorus ratio is desired for optimum growth (Pinckney et al., 2001). A higher ratio represents phosphorus limitation while a lower ratio represents nitrogen limitation. Because the previously derived nutrient loading model only contains orthophosphate and not total phosphorus, nitrogen will have to be assumed to be the limiting nutrient. This should hold true because nitrogen is typically the limiting nutrient in estuarine waters (Pinckney et al., 2001). The half saturation constant k_{sn} was chosen to be 12.5 mg m^{-3} based on the literature (Chapra, 1997).

The next step in creating this model was to determine the potential losses for phytoplankton within the canal. These potential losses include grazing by zooplankton, sedimentation, wash-out, and metabolic related losses. The previously discussed

flushing times will be used to calculate losses due to wash-out. Sedimentation rates involve sinking and resuspension of phytoplankton, but based on the literature this can be ignored in this model because the tidal movements and river flows of the estuary minimize this loss (Zison et al., 1979). The losses due to zooplankton were estimated based on previous studies that found these losses to average a rate of 0.53 d^{-1} in estuaries (Calbet and Landry, 2004). The metabolic losses include consumption of carbon for self-maintenance throughout the dark period of the night and losses due to decomposition. These rates were chosen to be 0.05 d^{-1} and 0.03 d^{-1} respectively based on the literature (Reynolds, 2006). The sum of the death rates was therefore calculated to be 0.61 d^{-1}. This average total was included with the flushing times to calculate the total losses within each segment.

Because light, temperature, and losses are considered constant rates in this model, the only time variable portion of the chlorophyll model is nitrogen concentration. Therefore the varying nitrogen concentrations had to be calculated in each of the four segments of the canal. To simulate nitrogen levels in the canal as a result of storm runoff three different loading scenarios were used. The first scenario was the average wet season loading. This scenario was run using step loading until a near steady state was reached. Once the steady state was reached a storm was then simulated using the loading averages from March of 2006. This was the month with the highest modeled loading into the Ala Wai from 2002-2009. Even though this is the highest monthly average it is still the average input for an entire month, and a single large storm event should produce higher average levels of runoff. This increased rate of

loading was modeled for 20 hours. At this time the nitrogen input was switched to reflect dry weather conditions. For this loading rates from May of 2009 were used. This is the driest month from the modeled eight year period and is meant to represent loading when there is no increased runoff from rain.

Because this model involves nutrient uptake it would not be appropriate to conservatively model the nitrogen concentrations in the canal. Laws et al. (1994) calculated that 70% of the organic inputs into the canal are respired. This was used as a rough estimate of available nutrient loss through respiration in the canal. The 70% loss was divided throughout the canal based on the total flushing time. These losses combined with the losses through flushing were used to model the decrease in nitrogen concentration once the storm hit.

Because step loading was used for this model the basic equation is similar to the step loading equation used in the nutrient modeling section with two differences. The first is that three different loading rates were used so the step loading functions had to be combined to obtain the concentration at any one point in time. The second is that the nitrogen was not treated as a conservative pollutant as stated above. Therefore a decay rate had to be added into the step loading function. The equation below was used to determine the nitrogen concentration of the first segment during the simulated period of high runoff. All of the variables listed are the same as those used in the nutrient modeling section. The new variables β and C_0 represent the rate of nitrogen consumption by respiration and the initial concentration of the wet season respectively.

$$c = \frac{W}{\lambda V}\left(1 - e^{-\lambda t}\right)\left(e^{-\beta}\right) + C_0$$

Segments 2-4 had the same added step that was discussed in the nutrient model where the loading from the previous segment also had to be included in the simulation. Adding in this loading rate gave the equation below where W_1 is the load that entered from the previous segment.

$$c = \{\frac{W}{\lambda V}\left(1 - e^{-\lambda t}\right) + \frac{W1}{\lambda V}\left(1 - e^{-\lambda t}\right)\}\left(e^{-\beta}\right) + C_0$$

Once the loading rate was dropped to that of dry weather the step loading function was no longer used as nitrogen concentration was no longer increasing. The equations used to simulate this loading period are similar to the delta function after a pulse input, but are not exactly the same as there is still a small nitrogen loading rate present from the rivers. The equation below was used to model the first segment. In this equation M is the mass of nitrogen that was present in segment 1 the previous hour minus the mass that flowed out to segment 2 due to flushing. The equations used for segments 2-4 were similar but again the loads from the previous segments were also added.

$$c = \frac{M + W}{V}\left(e^{-\beta}\right)\left(e^{-\lambda}\right)$$

The resulting model of total nitrogen concentrations within the canal can be seen in figure 13. In the figure the averages are set to the wet season averages at time 0 then the increased loading begins in the first hour. The high rate of loading from a modeled storm lasts for 20 hours until the loading is decreased to dry weather conditions.

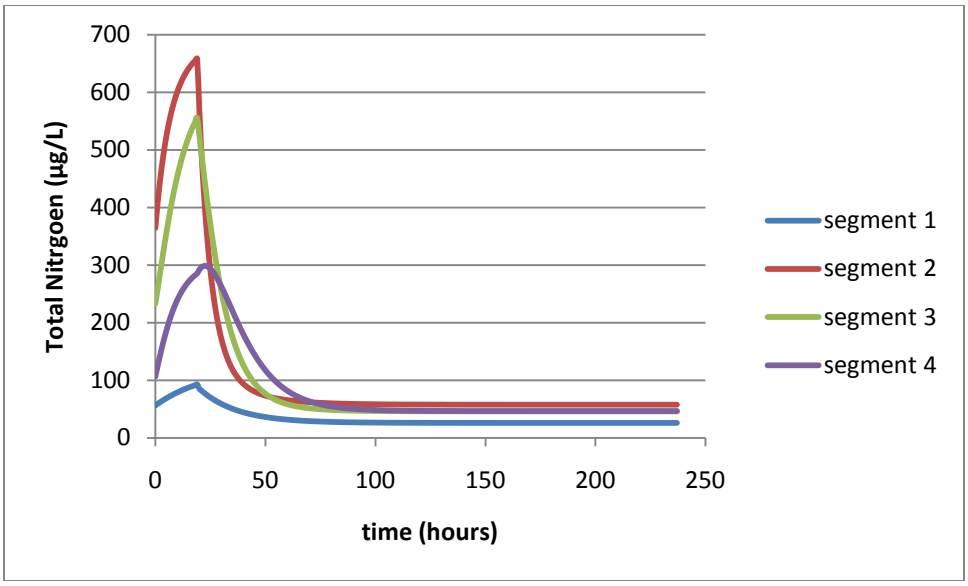

Figure 13. Modeled total nitrogen concentration as a result of storm runoff

The nitrogen data from the above figure was used in the time variable model of phytoplankton growth. The original phytoplankton concentrations used in each of the segments' growth models were determined from the dry weather chlorophyll averages measured and discussed in the field data section of this paper. Because the growth model is for phytoplankton the chlorophyll concentrations had to be converted to phytoplankton concentrations. Chlorophyll typically makes up about 2% of phytoplankton mass (Chapra, 1997) so the chlorophyll concentrations were multiplied by 50 to obtain an average phytoplankton concentration.

The mass of phytoplankton in any given segment was added to the mass of phytoplankton entering from the previous segment through flushing. This total mass was then divided by the volume of the segment to determine the concentration before any reaction. The derived concentration was then subject to either exponential growth or loss. The concentration increased if the growth rate minus the death rate was

greater than the rate of loss due to flushing. Likewise the concentration of phytoplankton decreased within that segment if the losses due to death and flushing exceeded that of growth. After the concentration of phytoplankton was determined it was then converted back to chlorophyll *a* concentration. The modeled chlorophyll *a* concentrations using the discussed parameters can be seen in figure 14.

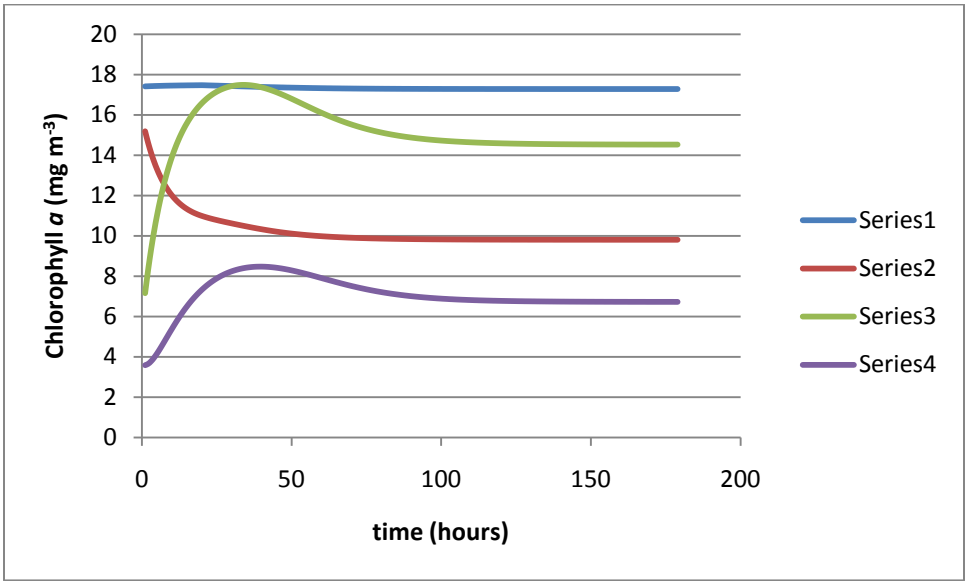

Figure 14. Chlorophyll concentrations based on modeled results using discussed parameters.

As can be seen in the model despite the large increase in nutrient concentrations the chlorophyll concentrations within the canal more or less stay the same and even decrease in the second segment. This does not match what was seen in the field or what is to be expected from an increase in nutrients. As previously discussed a lot of the parameters were estimated based on literature recommendations or past studies within the canal. It is clear that the current parameters do not accurately reflect the potential for growth within the canal based on field data. Two potential sources for

error are the growth rate which was estimated at 2 d^{-1} based on literature and the inhibition of growth due to light limitation.

The extinction coefficient used was a previously determined average for the canal, but it has been noted that light is much less of a limitation at the mouth of the canal. However it is unlikely to be the major factor affecting this model because when the maximum chlorophyll concentrations were measured high levels of suspended sediment clearly reduced the available light levels within the canal.

It is therefore likely that the temperature dependent growth rate parameter which was calculated to be 2.75 d^{-1} was underestimated. This had been calculated based on the assumption that the average growth at 20°C took place at a rate of 2 d^{-1}; however, higher rates have been reported (Zison et al., 1979). The model was therefore rerun with a k_g value of 3.5 d^{-1}. The chlorophyll concentrations resulting from this new growth rate can be seen in figure 15.

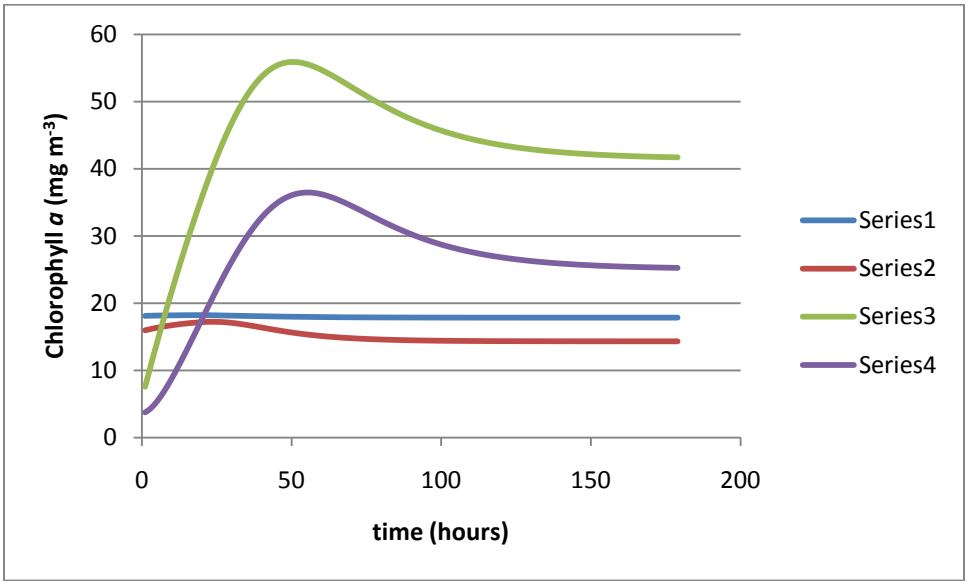

Figure 15. Chlorophyll concentration model with adjusted growth rate.

Chlorophyll Model/Data Discussion

The adjusted growth rate model agrees more closely with field data than does the original model. The actual field data shows nutrient concentrations with a slightly different pattern and greater values. It is important to note however that the field data measurements for segment 2 were taken at the border of segments 2 and 3. This may explain the discrepancy between the field data and modeled results for segment 2.

This model also does not incorporate the nutrient loading data from the series of storms that were the cause of the spike in chlorophyll measured in the field. The loading data from those storms is incomplete so they were not able to be used. It is therefore not the intent of this model to mirror those field conditions 100%, but rather to give a better understanding of the general increase in biological activity in the canal following a storm.

Both the field data and the model suggest that the greatest increases in biological activity following a storm will occur towards the mouth of the canal. This is in contrast to the dry weather chlorophyll averages which are greatest towards the head of the canal. The increase in production towards the mouth of the canal can be attributed to the large increase in nutrients following a rainstorm. Previous studies have documented that the levels of nitrogen and phosphorus are higher in the canal following rain events (Laws et al. 1994). Loading data used for this model has also shown that the greatest increase in these nutrients comes from via the Mānoa-Palolo Drainage Canal and Makiki Stream. It is therefore understandable the portions of the canal downstream of these outlets incur the greatest increase in productivity.

The reason why the head of the canal has a higher level of productivity during dry weather despite less nutrient inputs is potentially due to a longer flushing time. Past studies have shown that the water in segment one has a long residence time due to its depth relative to segment two (Gonzalez, 1971). Much of segment two is a meter or less deep because of sediment deposits from the Mānoa-Palolo Drainage Canal. Gonzalez concluded that water exchange behind this sediment deposit occurred irregularly and was driven in large part by a thermohaline process. This may mean that nutrients in this segment have a longer residence time than predicted by the fraction of freshwater flushing time method. It is possible that since the freshwater typically floats on the surface that it can more easily escape the segment than the bottom saline waters which may hold much of the nutrients. This could also explain why runoff is able to decrease the chlorophyll concentration within this segment. The increased mixing from a rain event may allow much of the nutrients and phytoplankton to leave this segment.

One final thing to take from these data is that the large increase in chlorophyll concentrations following an influx of nutrients from storm runoff suggests that previous assertions that nutrients in the canal are non-limiting are incorrect. The largest measured increase in chlorophyll levels occurred when suspended sediment levels were also at their highest. This is not to suggest that light is not limiting in any way in the canal because of course it is to some extent especially at deeper depths. However, it is important to recognize that increased nutrients from storm runoff can also play a large role in phytoplankton growth in the canal.

Wastewater Spill Model

Another potential use for the water quality model is to predict the contamination levels as a result of a wastewater spill such as the one that occurred in March of 2006. The suggestion here is not to replace field data monitoring of such a spill, but to show that a simple model such as this would give an estimate of when pollution levels would reach allowable amounts.

The model created for this paper is based on the spill that occurred in the Ala Wai in March of 2006. During the spill roughly 48 million gallons of raw wastewater were discharged into the Ala Wai over a six day period. These flow numbers were used to create the loading data of this model. The 48 million gallons over six days was converted into an hourly flow of 333,000 gallons per hour. This model uses fecal coliform populations and decay rates to estimate water quality levels after the spill. The ease of working with this water quality model is that any bacteria, flow, or decay rate can easily be switched in and out to quickly determine the likely population dynamics over time. It is assumed that the wastewater influent into the canal had a fecal coliform concentration of 10^8 bacteria liter^{-1}. The decay rate for the bacteria was chosen to be 0.6 d^{-1} based on previously studied field data (Kadlec & Knight, 1996).

The wastewater spill that occurred in 2006 fed directly into segment 2 of the water quality model. Because of this the bacterial concentrations will only be modeled for segments 2, 3, and 4. The loading that occurred into the second segment was treated as a constant so a step loading function was used to model the first six days of concentration within segment 2.

$$c = \frac{W}{\lambda V}\left(1 - e^{-\{(\lambda+\beta)t\}}\right)$$

After the six day period was over the decrease in concentration was modeled as a delta function with exponential decay.

$$c = c_0 e^{-(\lambda+\beta)}$$

The term c_0 represents the concentration of the segment in the previous hour. The concentrations of the next two segments were treated differently because their loading rates were time variable. These segments were modeled using exponential loading functions. The equation below was used to represent the concentration in the segments 3 and 4 after 1 hour. Each additional hour's concentration was determined by adding the concentration from this equation to the concentration from the previous hour minus its losses due to flushing and decay.

$$c = \frac{W}{V(\lambda+\beta)}\left(e^{-\beta} - e^{-\lambda}\right)$$

Using the parameters described above the concentration of fecal coliform was modeled against time for the simulated spill. The concentrations in the three segments can be seen in figure 16.

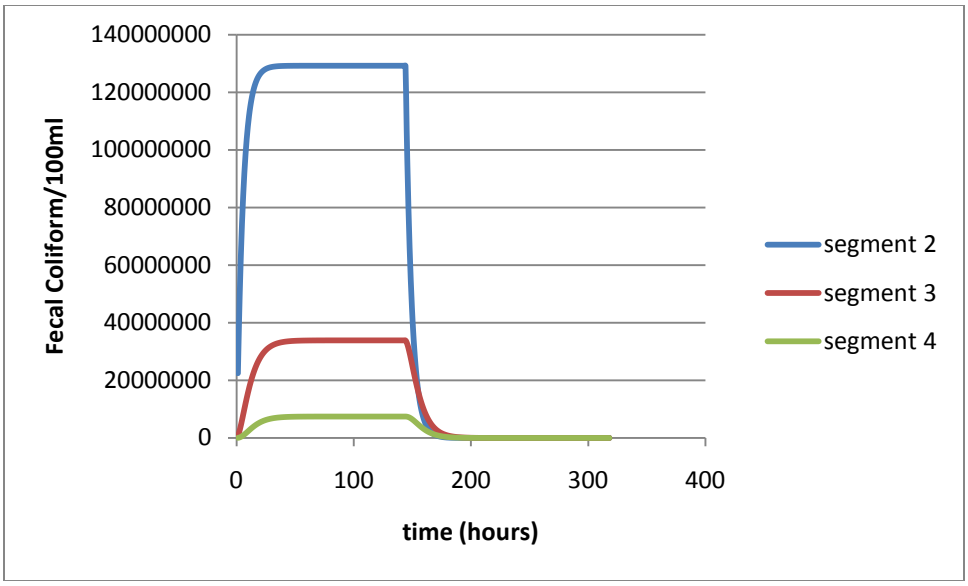

Figure 16. Modeled fecal coliform concentrations for segments 2, 3, and 4.

In 2006 the beaches around the Ala Wai Canal were reopened 6 days after the spill. This model does not include flow and transport of contaminants outside of the canal, but the numbers are still worth comparing to give a general idea of accuracy. 6 days after the modeled spill was turned off the concentrations of the three segments were 0.0001, 0.81, and 0.78 fecal coliform/100ml.

Hawai‘i does not actually use fecal coliform as a wastewater indicator because of its natural presence in the environment. For the purpose of this model that does not matter as the name could simply be removed and this model could represent any bacteria with a decay coefficient of 0.6 d^{-1}. For the most accurate use of this model the decay coefficient for a bacteria that Hawai‘i has standards for such as Enterococci should actually be tested in the environmental parameters of the Ala Wai Canal. Once a reliable decay coefficient is determined this model could be used to estimate cleanup time for any input parameters. Even without perfect input parameters this model is in general agreement with the 6 day closure of beaches in the areas surrounding the spill.

Conclusions

The modeled seasonal concentrations of total nitrogen were below the limit of the state's water quality standard of 200µg/L. However, the modeled concentrations exceeded this standard in segments 2 and 3 during the wet season and in segment 2 during the dry season. The water quality standard for total nitrogen also states the concentration should not exceed 500µg/L more than 2% of the time. A rainstorm was modeled using loading data from March of 2006. Using these data the concentrations of total nitrogen in segments 2 and 3 were modeled to exceed 500µg/L. The overall concentration of the canal, however, was modeled to be 279µg/L as a result of this storm loading.

The modeled seasonal concentrations of orthophosphate were 6.8µg/L and 4.8µg/L for the wet and dry seasons. It could not be determined if the water quality standard for total phosphorus was met because only orthophosphate data were available for modeling. Both seasonal orthophosphate concentrations do fall below the water quality standard for total phosphorus of 25µg/L.

Based on the water quality standards for the Ala Wai Canal the state of Hawai'i created Total Maximum Daily Loads (TMDLs) for nitrogen and phosphorus within the canal. It was determined that the standard of 25kg/day for total nitrogen was exceeded within the canal for both the wet and dry seasons in segments 2-4.

Using both the criteria of the water quality standards and total maximum daily loads the canal was modeled to have excess levels of nitrogen within certain segments. Segment 2 was consistently modeled to contain the highest concentration of the four

segments. One reason for this is because the largest nitrogen load into the canal occurs via the Mānoa-Palolo Drainage Canal which feeds directly into segment 2. The loading rates of total nitrogen through this source must be reduced for the nitrogen limits to be met within the canal.

Field data supported the modeled high concentrations of nutrients that followed a rainstorm. Chlorophyll *a* levels were shown to drastically increase towards the mouth of the canal after a rain event. Chlorophyll concentrations in segments 3 and 4 in particular showed the greatest level of increase with chlorophyll *a* concentrations 6.2 and 21.8 times greater than their dry weather averages. The increases in these later segments were attributed to the high levels of nutrient runoff via the Mānoa-Palolo drainage canal and Makiki Stream. This increase in productivity following an influx of nutrients refutes the notion that nutrients are non-limiting within the canal. The average chlorophyll *a* concentrations in the canal suggests that in dry weather the canal is slightly eutrophic, but that after a storm this problem becomes exacerbated.

From the extreme value method and methods described by Liu (1982) a biological rate constant was determined for each of the four segments. The ratio of the rate of respiration to the maximum rate of photosynthesis of each segment was the basis for the calculation of these biological rate constants. These ratios were calculated to be 0.42, 0.34, 0.25, and 0.17 for segments 1-4 respectively. The high ratios of segments 1 and 2 represent the fact that they are highly productive.

The four ratios of respiration rate and maximum rate of photosynthesis agree with the dry weather chlorophyll *a* data. Both sets of data point to the fact that the

segments nearest the head of the canal are highly productive during dry weather. The segments nearest the mouth of the canal also display fairly high levels of bioproductivity during dry weather, but not to the extent of segments 1 and 2. The equations for the extreme value method were not able to be used for wet weather conditions. However, the water quality model and field data for chlorophyll suggest that these levels of productivity would be even greater during wet conditions especially for the third and fourth segments.

One final application of the water quality model was discussed. The model was used to determine the fate of bacterial pollutants following a wastewater spill. The loading parameters from the spill that occurred in the canal in March of 2006 were used. Using the water quality model it was shown that the concentrations of bacteria in the canal would have been below required limits after 6 days. This is in general agreement with the timeline that was used by the city to reopen the surrounding beaches to the public.

References

Calbet, A., and M. R. Landry (2004), Phytoplankton growth, microzooplankton grazing and carbon cycling in marine systems, Limnol. Oceanogr., 49, 51–57.

Chapra, S.C. 1997. Surface Water-Quality Modeling. McGraw-Hill, New York.

Cloern, J.E. 2001. Review. Our evolving conceptual model of the coastal eutrophication problem. *Mar. Ecol. Prog. Ser. 210*, 223–253.

Duarte C.M., Conley D.J., Carstensen J., Sanchez-Comacho M. 2009. Return to Neverland: Shifting baselines affect eutrophication restoration targets. *Estuaries Coasts* 32:29–36

E.K. Noda and Associates, Inc. 1992. *Ala Wai Canal Improvement Project Feasibility Report*

Ekau, W., Auel, H., P¨ortner, H.O., Gilbert, D. 2010. Impacts of hypoxia on the structure and processes in pelagic communities (zooplankton, macro-invertebrates and fish). *Biogeosciences.* 7: 1669-1699

Freeman, William, 1993. Revised Total Maximum Daily Load Estimates for Six Water Quality Limited Segments, Island of Oahu, Hawai‘i. November, 1993.

Gonzalez, F. 1971. Descriptive Study of the Physical Oceanography of the Ala Wai Canal. M.S. thesis, University of Hawai‘i, Honolulu

Harris, C. 1972. Primary Production in a Small Tropical Estuary. M.S. thesis, University of Hawai‘i, Honolulu.

Hawai‘i Department of Health (HIDOH), 2002. Revisions to Total Maximum Daily Loads for the Ala Wai Canal, Oahu, Hawai‘i. June, 2002.

Kadlec, R.H. and R.L. Knight. 1996 Treatment Wetlands. CRC Press, Boca Raton

Lau, L.S., Mink, J.F., 2006. Hydrology of the Hawaiian Islands. University of Hawai'i Press, Honolulu.

Laws, E.A., Doliente, D., Hirayama, J., Hokama, M.L., Kim, K., Li, S., Minami, S., Morales, C., 1993. Hypereutrophication of the Ala Wai Canal, Oahu, Hawai‘i: Prospects for cleanup. Pacific Sci. 47, 59–75.

Laws, E.A., Hiraoka, J., Mura, M., Punu, B., Rust, T., Vink, S., Yamamura, C. 1994. Impact of Land Runoff on Water Quality in an Hawaiian Estuary. *Marine Environmental Research.* 38: 225-41.

Liu, C.C.K. 1982. Filtering of Dissolved Oxygen Data in Stream Water Quality Analysis. Water Resources Bulletin. February, 1982.

Mallin, M.A., M.H. Posey, M.R. McIver, D.C. Parsons, S.H. Ensign, T.D. Alphin. 2002. Impacts and recovery from multiple hurricanes in a Piedmont-coastal plain river system. *BioScience* 52: 999-1010.

Miller, J. N. 1975. Ecological Studies of the Biota of the Ala Wai Canal. University of Hawai'i, Hawai'i Institute of Geophysics Report HIG-75-8.

Montgomery, M.T., Coffin, R.B., Boyd, T.J., Hamdan, L.J., Smith, J.P., Plummer, R.E. Walker, S.E.,Dittel, A., Masutani, S.M., Li, Q.X., Osburn, C.L. 2009. Bacterial Production and Contamination Mineralization in Sediments of the Ala Wai Canal, Oahu, Hawai‘i. NavalResearch Lab, Washington DC

Odum, H.T., 1956. Primary production in flowing waters. *Limnol. Oceanogr.* 1: 102-117.

Pinckney, J. L., H. W. Paerl, P. Tester and T. L. Richardson, 2001. The role of nutrient loading and eutrophication in estuarine ecology. Environ. Health Perspect. 109, Supplement 5:699.

Reynolds, C.S. 2006. The Ecology of Phytoplankton. Cambridge University Press, New York

Wang, H., M. Hondzo, C. Xu, V. Poole, and A. Spacie. 2002. Dissolved oxygen dynamics of streams draining an urbanized and an agricultural catchment. *Ecological Modeling.* 160: 145-161

Wetzel, R.G. 2001. Limnology: Lakes and River Ecosystems, 3rd ed. Academic, San Diego.

Zison, S. W., K. F. Haven, & W. B. Mills, 1977. Water Quality Assessment: A Screening Method for Nondesignated 208 Areas, EPA-600/9-77-023, (U.S. Environmental Protection Agency, Athens, GA).

Zison, S.W., W.B. Mills, D. Deimer, and C.W. Chen, 1979. Rates, Constants, and Kinetics Formulations in Surface Water Quality Modeling. Published by U.S. EPA Environmental Research Laboratory, Athens, Georgia, EPA-600/3-78-105.

Appendix A: Salinity Profiles

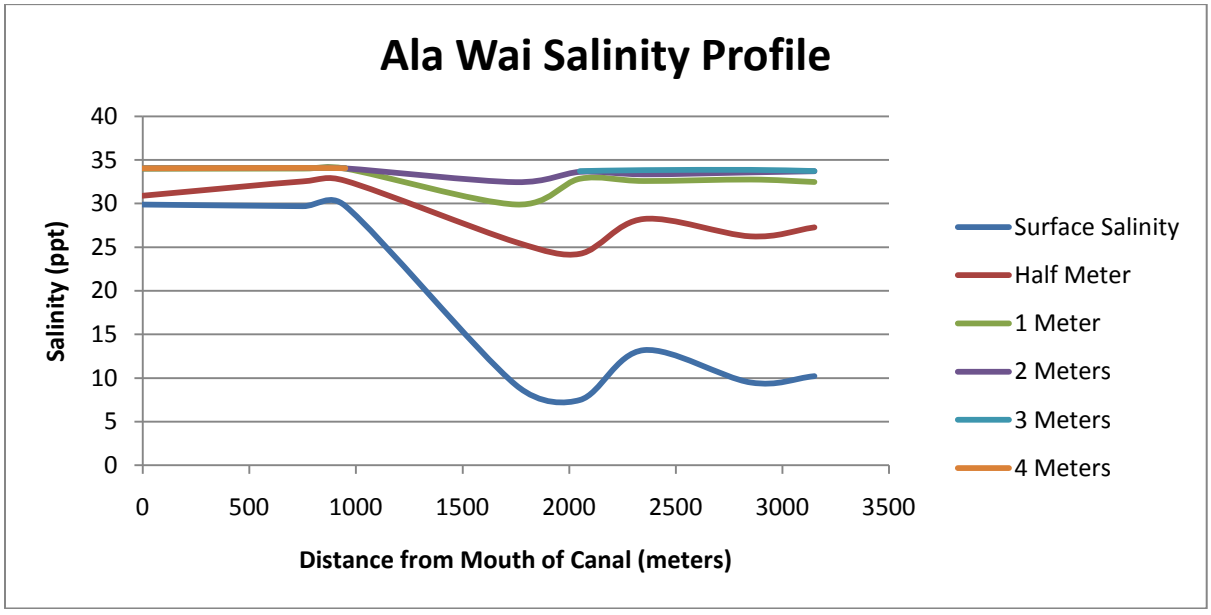

Figure A1. Dry season salinity profile measured for this study.

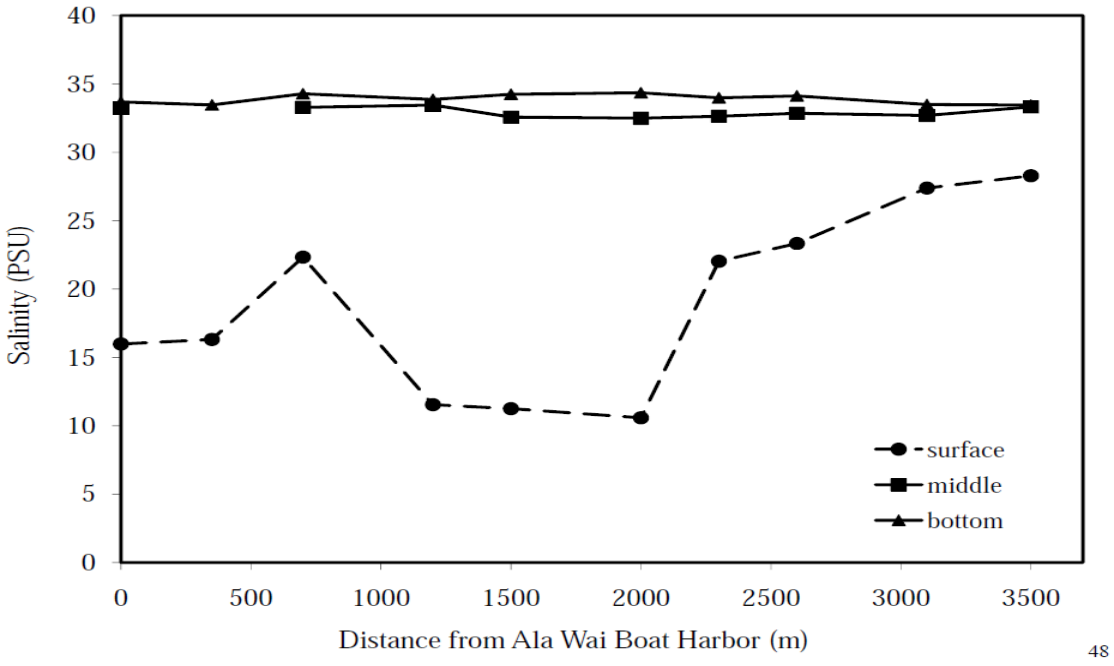

Figure A2. Wet weather salinity profile measured in 2003 by Naval Research Laboratory.

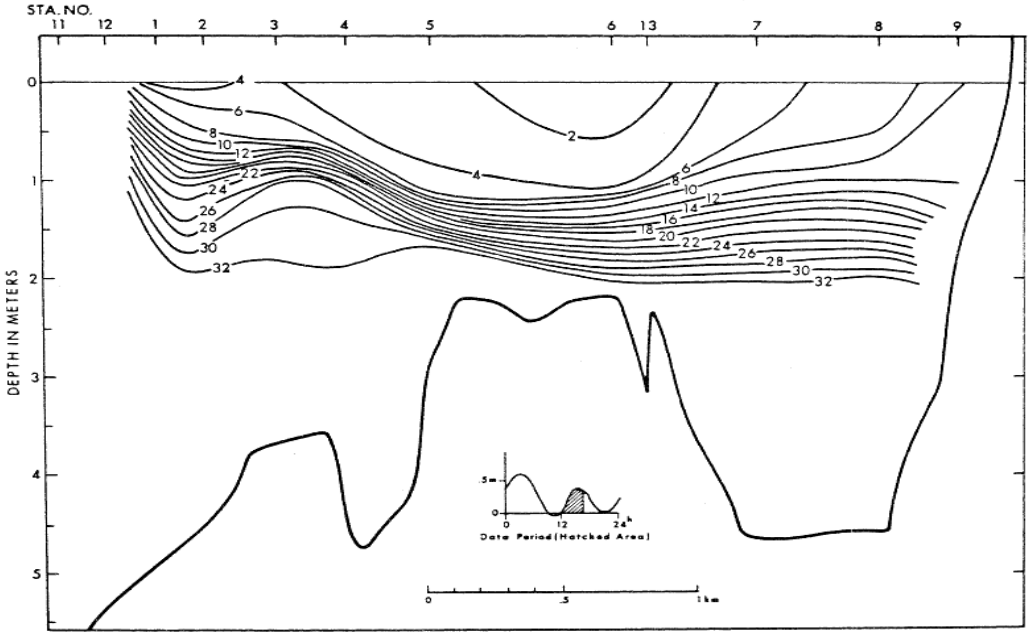

Figure A3. Salinity profile measured March 16, 1969 by Frank Gonzalez.

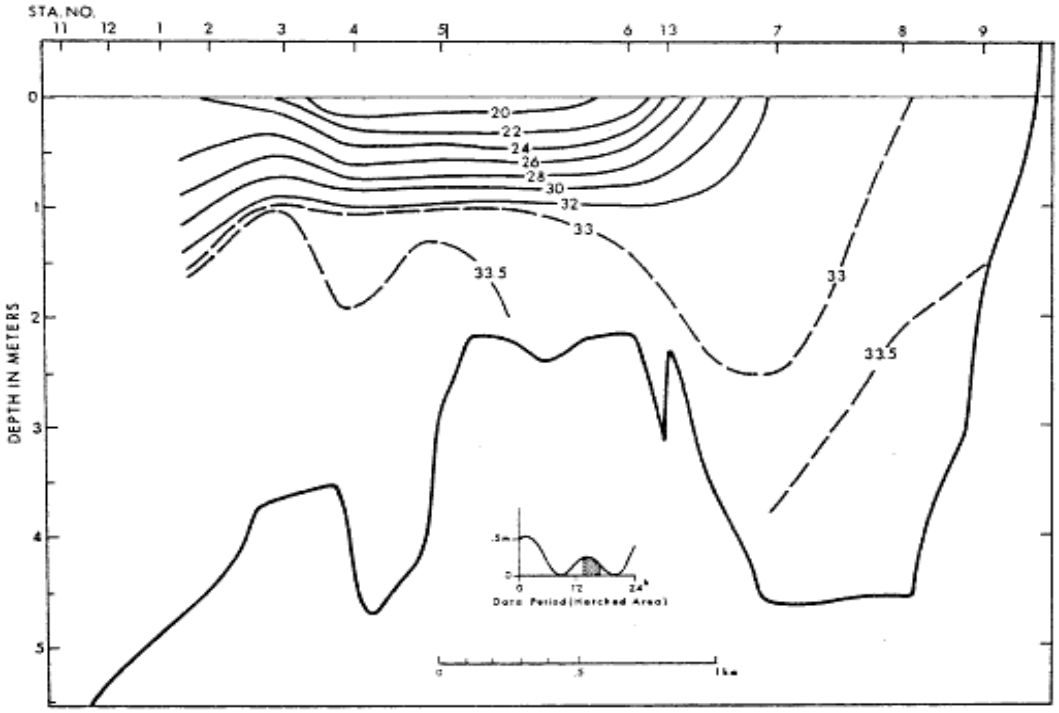

Figure A4. Salinity profile measured March 29, 1969 by Frank Gonzalez.

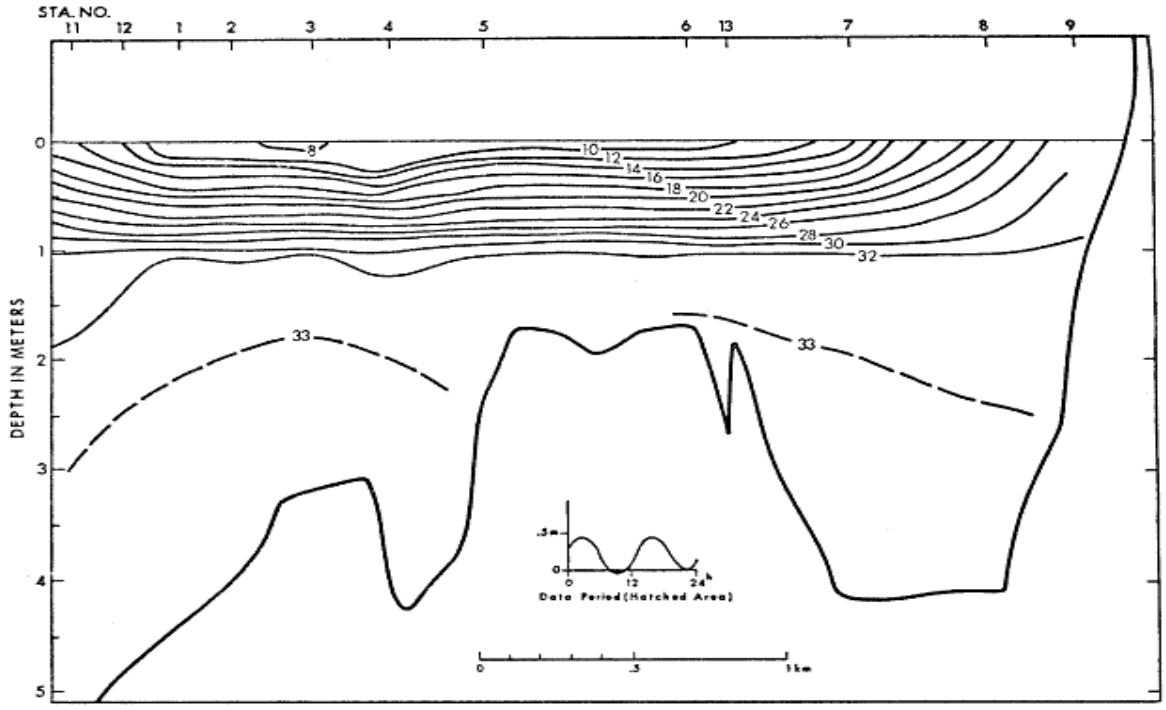

Figure A5. Salinity profile measured April 1, 1969 by Frank Gonzalez.

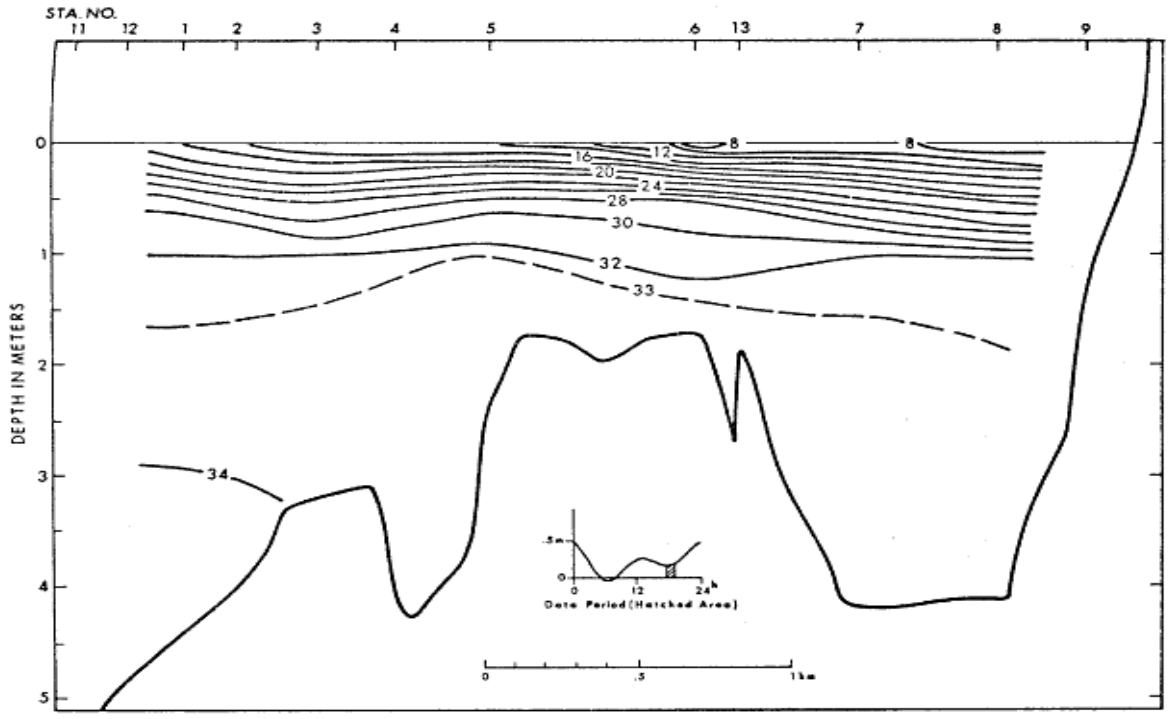

Figure A6. Salinity profile measured May 9, 1969 by Frank Gonzalez.

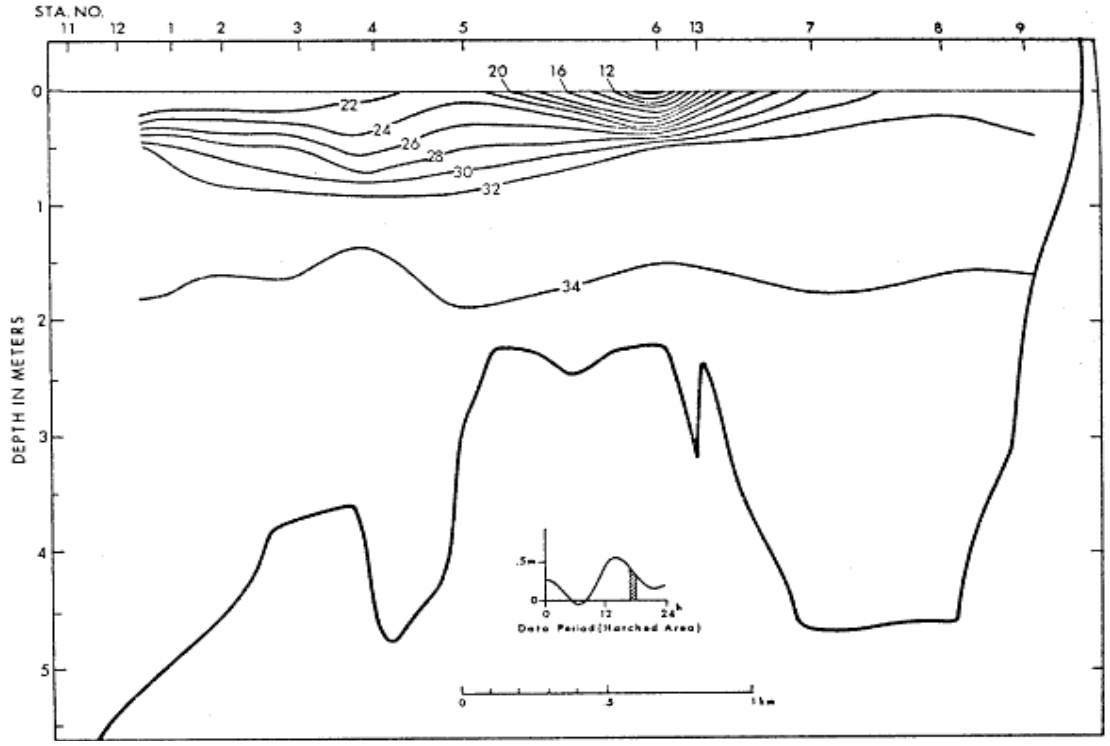

Figure A7. Salinity profile measured June 10, 1969 by Frank Gonzalez.

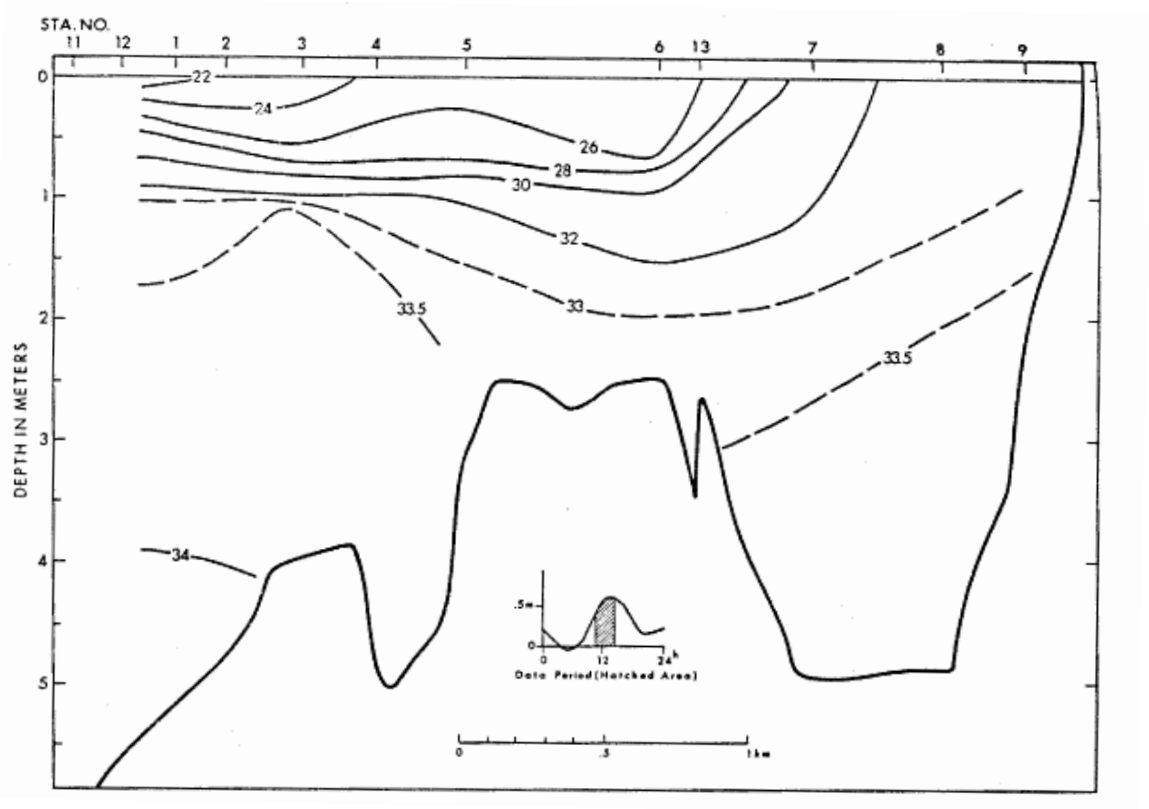

Figure A8. Salinity profile measured June 25, 1969 by Frank Gonzalez.

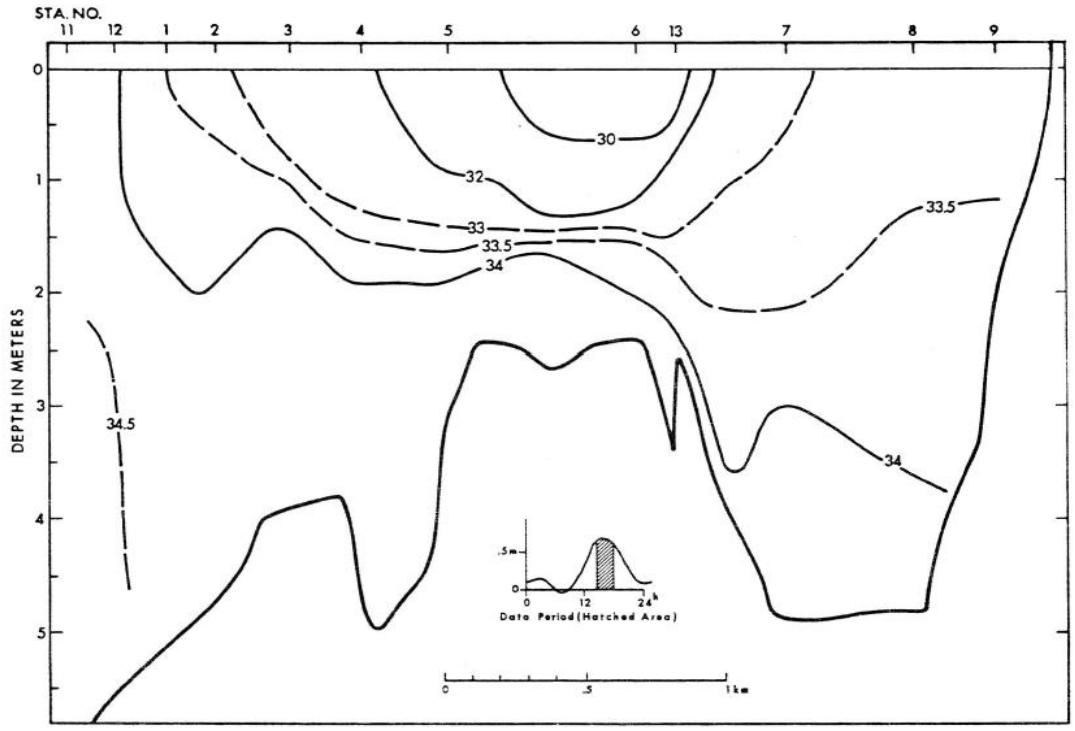

Figure A9. Salinity profile measured July 12, 1969 by Frank Gonzalez.

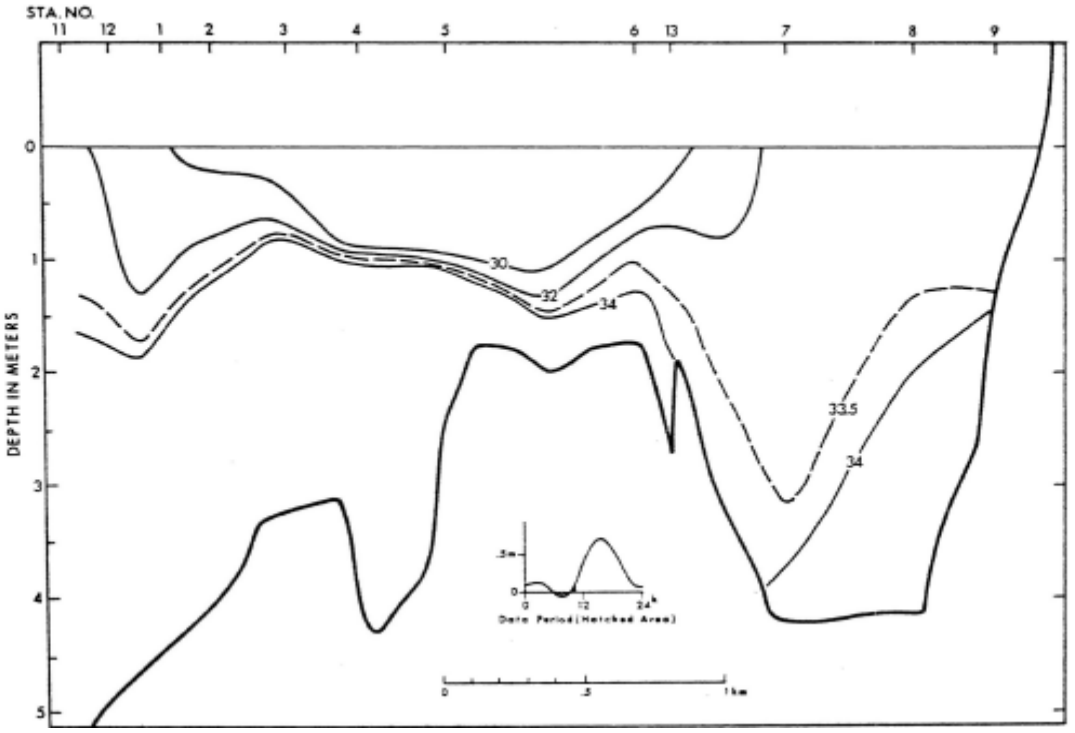

Figure A10. Salinity profile measured July 12, 1969 by Frank Gonzalez.

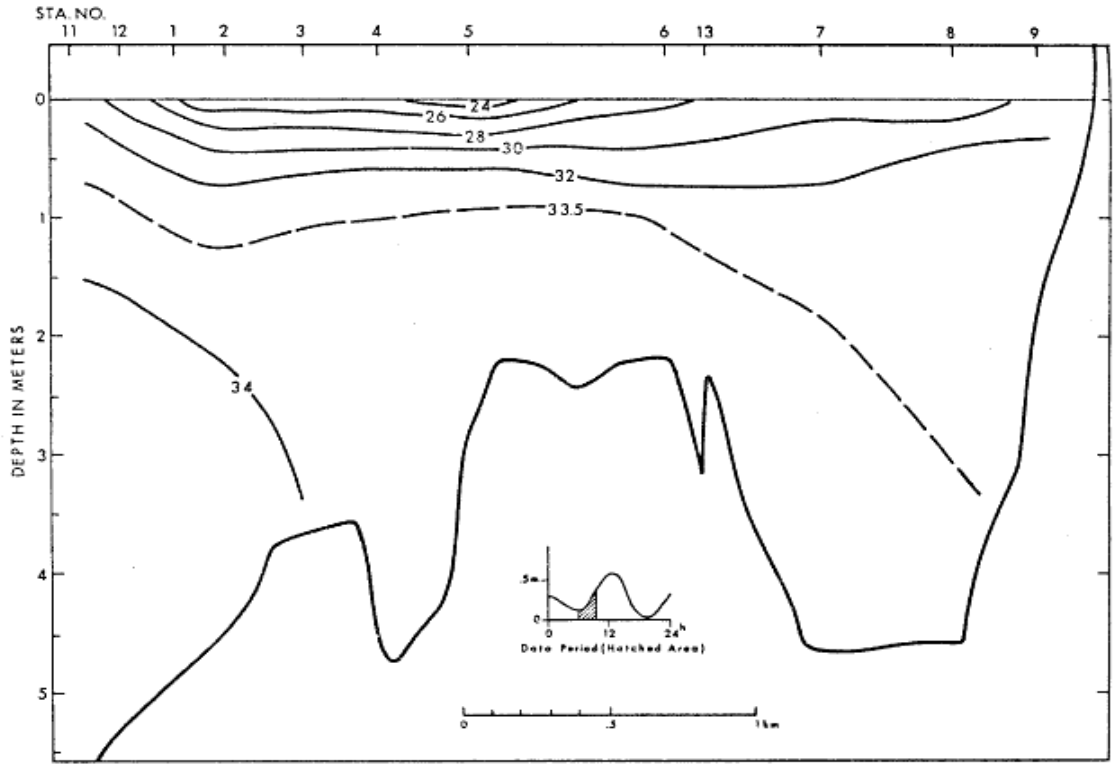

Figure A11. Salinity profile measured October 20, 1969 by Frank Gonzalez.

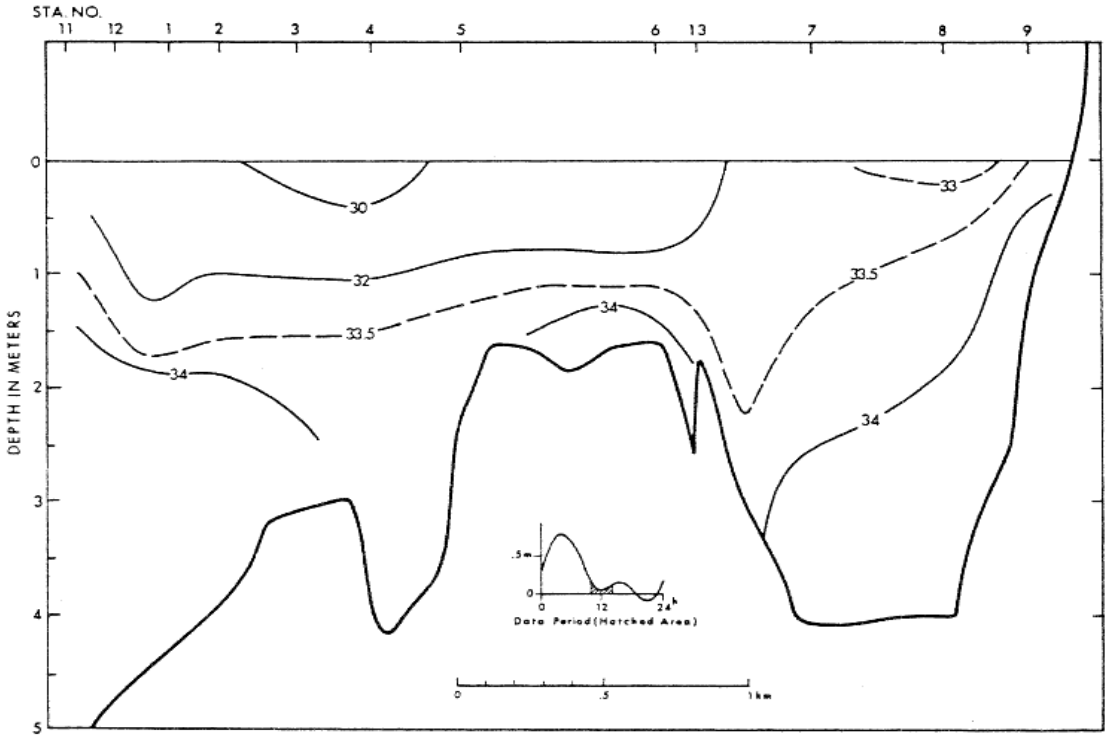

Figure A12. Salinity profile measured December 9th, 1969 by Frank Gonzalez.

Appendix B: Dissolved Oxygen Measurements

Table B1. Dissolved oxygen data from February 2, 2011. Data was collected in dry weather conditions during an outgoing tide.

Location	Time	Depth	Dissolved Oxygen (mg/l)
Segment 1	18:40	Surface	10.45
		0.5 meters	9.4
Segment 2	19:50	Surface	12.54
		0.5 meters	11.17
Segment 3	19:00	Surface	11.95
		1 Meter	8.86
		2 Meters	7.13
		3 Meters	6.67
Segment 4	19:25	Surface	12.07
		1 Meter	8.42
		2 Meters	7.29
		3 Meters	6.75

Table B2. Dissolved oxygen data from February 6, 2011. Data was collected in dry weather conditions during an outgoing tide.

Location	Time	Depth	Dissolved Oxygen (mg/l)
Segment 1	7:00	Surface	5.65
		0.5 meters	4.65
Segment 2	6:45	Surface	8.68
		0.5 meters	8.52
Segment 3	6:15	Surface	8.19
		1 Meter	6.88
		2 Meters	5.90
		3 Meters	5.61
Segment 4	6:25	Surface	8.60
		1 Meter	7.32
		2 Meters	5.91
		3 Meters	5.68

Table B3. Dissolved oxygen data from the morning of February 10, 2011. Data was collected in dry weather conditions during an incoming tide.

Location	Time	Depth	Dissolved Oxygen (mg/l)
Segment 1	6:45	Surface	7.42
		0.5 meters	5.01
Segment 2	6:25	Surface	4.78
		0.5 meters	3.44
Segment 3	6:00	Surface	6.17
		1 Meter	6.13
		2 Meters	4.94
		3 Meters	4.52
Segment 4	6:10	Surface	6.72
		1 Meter	6.39
		2 Meters	5.60
		3 Meters	4.82

Table B4. Dissolved oxygen data from the evening of February 10, 2011. Data was collected in dry weather conditions during an incoming tide.

Location	Time	Depth	Dissolved Oxygen (mg/l)
Segment 1	17:20	Surface	11.94
		0.5 meters	11.62
Segment 2	18:00	Surface	7.16
		0.5 meters	7.18
Segment 3	17:30	Surface	6.87
		1 Meter	6.26
		2 Meters	5.57
		3 Meters	4.17
Segment 4	17:40	Surface	7.29
		1 Meter	7.27
		2 Meters	6.00
		3 Meters	4.81

Table B5. Dissolved oxygen data from February 11, 2011. Data was collected during wet weather conditions and during an incoming tide.

Location	Time	Depth	Dissolved Oxygen (mg/l)
Segment 1	17:45	Surface	5.56
Segment 2	18:30	Surface	6.88
		0.5 meters	7.29
Segment 3	18:00	Surface	7.16
		1 Meter	6.41
		2 Meters	4.90
		3 Meters	4.68
Segment 4	18:10	Surface	7.75
		1 Meter	6.41
		2 Meters	4.90
		3 Meters	4.68

Table B6. Dissolved oxygen data from the morning of February 12, 2011. Data was collected during wet weather conditions and during an outgoing tide.

Location	Time	Depth	Dissolved Oxygen (mg/l)
Segment 1	7:20	Surface	4.83
Segment 2	7:05	Surface	5.69
Segment 3	6:30	Surface	7.19
		1 Meter	4.99
		2 Meters	3.39
		3 Meters	3.86
Segment 4	6:50	Surface	6.39
		1 Meter	5.53
		2 Meters	4.23
		3 Meters	3.88

Table B7. Dissolved oxygen data from the afternoon of February 12, 2011. Data was collected during wet weather conditions and during an outgoing tide.

Location	Time	Depth	Dissolved Oxygen (mg/l)
Segment 1	12:50	Surface	3.44
Segment 2	13:40	Surface	6.55
Segment 3	13:00	Surface	6.64
		1 Meter	5.89
		2 Meters	5.37
		3 Meters	4.23
Segment 4	13:20	Surface	6.38
		1 Meter	5.83
		2 Meters	5.50
		3 Meters	4.45

Table B8. Dissolved oxygen data from the evening of February 12, 2011. Data was collected during wet weather conditions and during an incoming tide.

Location	Time	Depth	Dissolved Oxygen (mg/l)
Segment 1	18:00	Surface	4.32
Segment 2	18:50	Surface	7.65
		0.5 meters	6.78
Segment 3	18:15	Surface	7.19
		1 Meter	6.57
		2 Meters	5.85
		3 Meters	4.58
Segment 4	18:30	Surface	7.13
		1 Meter	6.60
		2 Meters	6.24
		3 Meters	4.75

Table B9. Dissolved oxygen data from the morning of February 13, 2011. Data was collected during wet weather conditions and during an outgoing tide.

Location	Time	Depth	Dissolved Oxygen (mg/l)
Segment 1	7:20	Surface	4.19
Segment 2	7:10	Surface	4.83
Segment 3	6:40	Surface	4.29
		1 Meter	4.11
		2 Meters	3.61
		3 Meters	3.41
Segment 4	6:50	Surface	4.93
		1 Meter	4.35
		2 Meters	3.95
		3 Meters	3.66

Table B10. Dissolved oxygen data from the afternoon of February 13, 2011. Data was collected during wet weather conditions and during an outgoing tide.

Location	Time	Depth	Dissolved Oxygen (mg/l)
Segment 1	12:40	Surface	5.78
Segment 2	13:25	Surface	7.49
Segment 3	12:55	Surface	5.87
		1 Meter	4.98
		2 Meters	4.28
		3 Meters	4.02
Segment 4	13:10	Surface	6.03
		1 Meter	5.83
		2 Meters	4.65
		3 Meters	4.26

Table B11. Dissolved oxygen data from the morning of February 16, 2011. Data was collected during dry weather conditions and an outgoing tide.

Location	Time	Depth	Dissolved Oxygen (mg/l)
Segment 1	7:20	Surface	4.12
Segment 2	7:10	Surface	7.12
		0.5 meters	6.52
Segment 3	6:40	Surface	6.93
		1 Meter	6.70
		2 Meters	6.71
		3 Meters	6.70
Segment 4	6:50	Surface	7.29
		1 Meter	7.02
		2 Meters	7.00
		3 Meters	6.93

Table B12. Dissolved oxygen data from the afternoon of February 16, 2011. Data was collected during dry weather conditions and an incoming tide.

Location	Time	Depth	Dissolved Oxygen (mg/l)
Segment 1	12:50	Surface	8.26
Segment 2	12:40	Surface	8.52
		0.5 meters	8.21
Segment 3	13:05	Surface	8.12
		1 Meter	7.76
		2 Meters	7.07
		3 Meters	6.96
Segment 4	13:15	Surface	8.67
		1 Meter	7.91
		2 Meters	7.32
		3 Meters	7.22

Table B13. Dissolved oxygen data from February 17, 2011. Data was collected during dry weather conditions and an outgoing tide.

Location	Time	Depth	Dissolved Oxygen (mg/l)
Segment 1	17:45	Surface	6.71
Segment 2	18:00	Surface	7.66
Segment 3	18:15	Surface	8.30
		1 Meter	8.90
		2 Meters	6.61
		3 Meters	6.33
Segment 4	18:20	Surface	8.18
		1 Meter	9.01
		2 Meters	7.20
		3 Meters	6.50

Table B14. Dissolved oxygen data from the morning of February 18, 2011. Data was collected during dry weather conditions and an outgoing tide.

Location	Time	Depth	Dissolved Oxygen (mg/l)
Segment 1	6:50	Surface	6.21
		1 meter	4.68
Segment 2	7:30	Surface	7.02
		0.5 meters	4.56
Segment 3	7:00	Surface	6.78
		1 Meter	5.70
		2 Meters	5.22
		3 Meters	5.17
Segment 4	7:10	Surface	7.28
		1 Meter	6.41
		2 Meters	5.74
		3 Meters	5.72

Table B15. Dissolved oxygen data from the evening of February 18, 2011. Data was collected during dry weather conditions and an outgoing tide.

Location	Time	Depth	Dissolved Oxygen (mg/l)
Segment 1	17:50	Surface	7.12
		1 meter	6.81
Segment 2	18:30	Surface	8.21
		0.5 meters	6.47
Segment 3	18:05	Surface	8.37
		1 Meter	8.04
		2 Meters	6.93
		3 Meters	5.54
Segment 4	18:15	Surface	8.09
		1 Meter	7.71
		2 Meters	6.92
		3 Meters	5.77

Table B16. Dissolved oxygen data from the morning of February 19, 2011. Data was collected during dry weather conditions and an outgoing tide.

Location	Time	Depth	Dissolved Oxygen (mg/l)
Segment 1	7:00	Surface	5.05
		1 meter	4.59
Segment 2	7:40	Surface	6.13
		0.5 meters	5.41
Segment 3	7:15	Surface	6.80
		1 Meter	5.66
		2 Meters	5.26
		3 Meters	5.43
Segment 4	7:20	Surface	7.16
		1 Meter	6.08
		2 Meters	5.59
		3 Meters	5.72

Table B17. Dissolved oxygen data from the afternoon of February 19, 2011. Data was collected during dry weather conditions and an incoming tide.

Location	Time	Depth	Dissolved Oxygen (mg/l)
Segment 1	13:25	Surface	7.09
Segment 2	14:35	Surface	8.94
		0.5 meters	8.67
Segment 3	13:40	Surface	7.50
		1 Meter	5.98
		2 Meters	5.71
		3 Meters	5.48
Segment 4	13:50	Surface	8.05
		1 Meter	7.09
		2 Meters	5.80
		3 Meters	5.63

Table B18. Dissolved oxygen data from the evening of February 19, 2011. Data was collected during dry weather conditions and an outgoing tide.

Location	Time	Depth	Dissolved Oxygen (mg/l)
Segment 1	18:25	Surface	8.45
		1 meter	7.83
Segment 2	19:00	Surface	8.55
		0.5 meters	7.81
Segment 3	18:40	Surface	7.54
		1 Meter	8.85
		2 Meters	7.22
		3 Meters	6.49
Segment 4	18:45	Surface	7.85
		1 Meter	8.12
		2 Meters	7.22
		3 Meters	6.55

Table B19. Dissolved oxygen data from the morning of February 20, 2011. Data was collected during wet weather conditions and an outgoing tide.

Location	Time	Depth	Dissolved Oxygen (mg/l)
Segment 1	6:45	Surface	6.34
		1 meter	4.78
Segment 2	7:20	Surface	7.45
		0.5 meters	4.80
Segment 3	7:00	Surface	7.08
		1 Meter	5.63
		2 Meters	5.47
		3 Meters	5.39
Segment 4	7:05	Surface	7.24
		1 Meter	5.81
		2 Meters	5.68
		3 Meters	5.63

Table B20. Dissolved oxygen data from the afternoon of February 20, 2011. Data was collected during wet weather conditions and an incoming tide.

Location	Time	Depth	Dissolved Oxygen (mg/l)
Segment 1	13:35	Surface	5.41
		1 meter	4.18
Segment 2	14:15	Surface	7.44
		0.5 meters	6.13
Segment 3	13:50	Surface	7.39
		1 Meter	4.92
		2 Meters	4.76
		3 Meters	4.79
Segment 4	14:00	Surface	7.63
		1 Meter	5.31
		2 Meters	4.95
		3 Meters	5.01

Table B21. Dissolved oxygen data from the evening of February 20, 2011. Data was collected during wet weather conditions and an outgoing tide.

Location	Time	Depth	Dissolved Oxygen (mg/l)
Segment 1	17:30	Surface	6.65
		1 meter	5.69
Segment 2	18:10	Surface	6.83
		0.5 meters	6.52
Segment 3	17:45	Surface	7.05
		1 Meter	6.17
		2 Meters	5.81
		3 Meters	5.49
Segment 4	17:50	Surface	7.32
		1 Meter	6.47
		2 Meters	5.83
		3 Meters	5.20

Table B22. Dissolved oxygen data from the morning of February 21, 2011. Data was collected during wet weather conditions and an outgoing tide.

Location	Time	Depth	Dissolved Oxygen (mg/l)
Segment 1	6:45	Surface	4.23
		1 meter	2.61
		1.5 meters	1.71
Segment 2	7:25	Surface	5.18
		0.5 meters	2.71
Segment 3	7:00	Surface	6.34
		1 Meter	5.22
		2 Meters	5.04
		3 Meters	4.52
		4 Meters	3.96
Segment 4	7:10	Surface	5.36
		1 Meter	5.10
		2 Meters	4.49
		3 Meters	4.30

Table B23. Dissolved oxygen data from the afternoon of February 21, 2011. Data was collected during wet weather conditions and an incoming tide.

Location	Time	Depth	Dissolved Oxygen (mg/l)
Segment 1	12:20	Surface	5.85
		1 meter	2.78
Segment 2	13:00	Surface	6.00
Segment 3	12:35	Surface	5.88
		1 Meter	4.75
		2 Meters	4.71
		3 Meters	3.69
		4 Meters	3.27
Segment 4	12:45	Surface	6.08
		1 Meter	4.91
		2 Meters	4.64
		3 Meters	3.77

Table B24. Dissolved oxygen data from the evening of February 25, 2011. Data was collected during dry weather conditions and an incoming tide.

Location	Time	Depth	Dissolved Oxygen (mg/l)
Segment 1	17:55	Surface	8.59
		1 meter	7.82
Segment 2	18:45	Surface	9.89
Segment 3	18:20	Surface	9.73
		1 Meter	9.53
		2 Meters	9.39
		3 Meters	8.58
Segment 4	18:30	Surface	9.95
		1 Meter	11.07
		2 Meters	10.65
		3 Meters	9.55

Table B25. Dissolved oxygen data from the morning of February 26, 2011. Data was collected during dry weather conditions and an outgoing tide.

Location	Time	Depth	Dissolved Oxygen (mg/l)
Segment 1	6:50	Surface	7.02
		1 meter	4.19
Segment 2	7:30	Surface	7.94
Segment 3	7:00	Surface	7.98
		1 Meter	7.18
		2 Meters	6.70
		3 Meters	6.06
Segment 4	7:10	Surface	7.87
		1 Meter	7.34
		2 Meters	6.68
		3 Meters	6.10

Table B26. Dissolved oxygen data from the afternoon of February 26, 2011. Data was collected during dry weather conditions and an outgoing tide.

Location	Time	Depth	Dissolved Oxygen (mg/l)
Segment 1	14:05	Surface	11.97
		1 meter	7.07
Segment 2	14:40	Surface	12.15
Segment 3	14:20	Surface	11.76
		1 Meter	9.61
		2 Meters	8.27
		3 Meters	6.81
Segment 4	14:30	Surface	12.12
		1 Meter	9.87
		2 Meters	8.21
		3 Meters	7.04

Table B27. Dissolved oxygen data from the evening of February 26, 2011. Data was collected during dry weather conditions and an incoming tide.

Location	Time	Depth	Dissolved Oxygen (mg/l)
Segment 1	17:40	Surface	9.25
		1 meter	8.45
Segment 2	18:20	Surface	11.09
Segment 3	17:55	Surface	11.81
		1 Meter	11.29
		2 Meters	9.62
		3 Meters	6.58
Segment 4	18:00	Surface	11.62
		1 Meter	10.50
		2 Meters	8.60
		3 Meters	7.25

Table B28. Dissolved oxygen data from the afternoon of February 27, 2011. Data was collected during dry weather conditions and an incoming tide.

Location	Time	Depth	Dissolved Oxygen (mg/l)
Segment 1	12:10	Surface	10.42
		1 meter	7.72
Segment 2	12:50	Surface	10.45
Segment 3	12:30	Surface	9.90
		1 Meter	7.69
		2 Meters	6.81
		3 Meters	6.49
Segment 4	12:35	Surface	10.41
		1 Meter	8.51
		2 Meters	7.72

Appendix C: Chlorophyll *a* Measurements

Table C1. Chlorophyll *a* concentrations from February 6, 2011. Measurements were taken during an outgoing tide.

Location	Chlorophyll a concentration (mg/m^3)
Segment 1	17.80
Segment 2	47.93
Segment 3	5.93
Segment 4	3.56

Table C2. Chlorophyll *a* concentrations from February 12, 2011. Measurements were taken during an outgoing tide.

Location	Chlorophyll a concentration (mg/m^3)
Segment 1	5.09
Segment 2	4.41
Segment 3	3.99
Segment 4	2.88

Table C3. Chlorophyll *a* concentrations from February 13, 2011. Measurements were taken during an outgoing tide.

Location	Chlorophyll a concentration (mg/m^3)
Segment 1	10.57
Segment 2	14.25
Segment 3	9.77
Segment 4	3.11

Table C4. Chlorophyll *a* concentrations from February 16, 2011. Measurements were taken during an outgoing tide.

Location	Chlorophyll a concentration (mg/m^3)
Segment 1	12.48
Segment 2	5.50
Segment 3	4.07
Segment 4	5.49

Table C5. Chlorophyll *a* concentrations from March 20, 2011. Measurements were taken during an incoming tide.

Location	Chlorophyll a concentration (mg/m^3)
Segment 1	14.47
Segment 2	9.90
Segment 3	5.47
Segment 4	5.31

Table C6. Chlorophyll *a* concentrations from March 21, 2011. Measurements were taken during an outgoing tide.

Location	Chlorophyll a concentration (mg/m^3)
Segment 1	11.82
Segment 2	12.40
Segment 3	3.19
Segment 4	2.09

Table C7. Chlorophyll *a* concentrations from March 22, 2011. Measurements were taken during an outgoing tide.

Location	Chlorophyll a concentration (mg/m^3)
Segment 1	27.42
Segment 2	23.23
Segment 3	6.14
Segment 4	4.07

Table C8. Chlorophyll *a* concentrations from March 23, 2011. Measurements were taken during an outgoing tide.

Location	Chlorophyll a concentration (mg/m^3)
Segment 1	40.17
Segment 2	15.29
Segment 3	5.53
Segment 4	3.60

Table C9. Chlorophyll *a* concentrations from March 24, 2011. Measurements were taken during an outgoing tide.

Location	Chlorophyll a concentration (mg/m^3)
Segment 1	20.08
Segment 2	9.63
Segment 3	7.21
Segment 4	3.74

Table C10. Chlorophyll *a* concentrations from March 25, 2011. Measurements were taken during an incoming tide.

Location	Chlorophyll a concentration (mg/m^3)
Segment 1	22.44
Segment 2	10.52
Segment 3	10.45
Segment 4	6.31

Table C11. Chlorophyll *a* concentrations from March 26, 2011. Measurements were taken during an incoming tide.

Location	Chlorophyll a concentration (mg/m^3)
Segment 1	14.59
Segment 2	36.08
Segment 3	31.32
Segment 4	59.48

Table C12. Chlorophyll *a* concentrations from March 27, 2011. Measurements were taken during an incoming tide.

Location	Chlorophyll a concentration (mg/m^3)
Segment 1	6.89
Segment 2	91.78
Segment 3	67.20
Segment 4	169.98